Parameterization of invariant manifolds for periodic orbits(I): efficient numerics via the Floquet normal form

Roberto Castelli * Jean-Philippe Lessard† J.D. Mireles James ‡

February 18, 2014

Abstract

We present an efficient numerical method for computing Fourier-Taylor expansions of stable/unstable manifolds associated with hyperbolic periodic orbits. Three features of the method are (1) that we obtain accurate representation of the invariant manifold as well as the dynamics on the manifold, (2) that the method admits natural a-posteriori error analysis, and (3) that the method does not require numerical integrating the vector field. Our method is based on the Parameterization Method for invariant manifolds, and studies a certain partial differential equation which characterizes a chart map of the (un)stable manifold. The method requires only that some mild non-resonance conditions hold between the Floquet multipliers of the periodic orbit. The novelty of the the present work is that we exploit the Floquet normal form in order to efficiently compute the Fourier-Taylor expansion. We present a number of example computations, including stable/unstable manifolds in phase space dimension as hight as ten, computation of manifolds which are two and three dimensional, and computation of some homoclinic connecting orbits.

1 Introduction

Equilibria and periodic orbits of nonlinear systems are building blocks for understanding global dynamics. The basins of attraction, repulsion, and stable/unstable manifolds associated with these building blocks provide information about how phase space fits together. The equilibria and periodic orbits together with their stable/unstable manifolds form an invariant skeleton which governs transitions from one region of phase space to another, describe where mixing and stagnation occur, and even establish the existence and whereabouts of chaotic motions. Given a particular nonlinear systems it is often difficult to represent periodic orbits and their invariant manifolds in closed form, hence substantial effort has gone into developing numerical methods for approximating these objects.

In this paper we present an efficient scheme for computing numerical approximations of local stable/unstable manifolds associated with hyperbolic periodic orbits of differential equations. The inputs to the method are a Fourier approximation for the periodic orbit *in*

*BCAM - Basque Center for Applied Mathematics, Bizkaia Technology Park, 48160 Derio, Bizkaia, SPAIN. Email: rcastelli@bcamath.org.

†**Corresponding author**. Université Laval, Département de Mathématiques et de Statistique, Pavillon Alexandre-Vachon, 1045 avenue de la Médecine, Québec, QC, G1V 0A6, CANADA and BCAM - Basque Center for Applied Mathematics, Bizkaia Technology Park, 48160 Derio, Bizkaia, SPAIN. Email: jean-philippe.lessard@mat.ulaval.ca.

‡Rutgers University. Email: jmireles@math.rutgers.edu.

addition to a Fourier approximation of the Floquet normal form. The method developed here applies to hyperbolic periodic orbits under mild non-resonance assumptions on the Floquet multipliers.

In order to illustrate some results which are obtained using our method we include Figures 1 and 2 in the present introductory section. The figures show the local stable and unstable invariant manifolds associated with a saddle periodic orbit on the global chaotic attractor of the Lorenz system (see Equation (20)) at the classical parameter values.

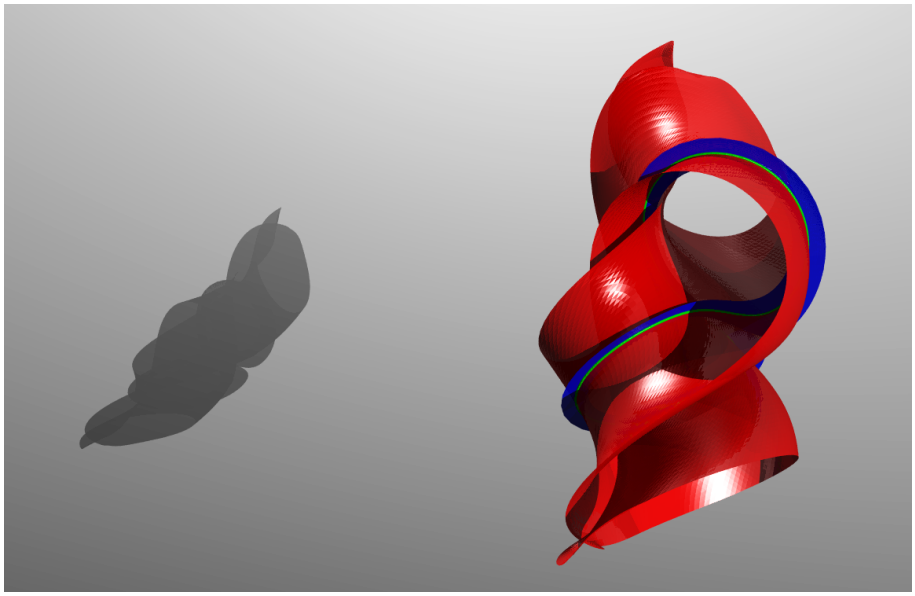

Figure 1: Local stable (red) and unstable (blue) manifolds associated with a hyperbolic periodic orbit (green) in the Lorenz attractor. This computation is carried out for the classical parameter values of $\rho = 28, \sigma = 10, \beta = 8/3$. The Figure illustrates the images of parameterizations truncated to Taylor order $N = 25$ and $M = 66$ Fourier Modes. No integration is performed in order to globalize the manifold. The stable manifold is not the graph of a function over the stable linear bundle of the periodic orbit. This highlights an important feature that the Parameterization Method which is that it can follow folds in the manifolds. The figure also illustrates the stretching and folding of the phase space near the periodic orbit.

Our method is based on the *Parametrization Method* introduced in [45, 46, 47]. Following the cited work, the idea is to study an *invariance equation* describing the invariant manifold. One plugs a certain formal series into the invariance equation and solves the problem via a power matching scheme. As we will show, this procedure leads to the a sequence of linear ordinary differential equations with periodic coefficients which then need to be solved recursively.

From the theoretical point of view the existence of solutions for these equations is well understood provided certain resonance conditions are satisfied. Abstract convergence of the Fourier-Taylor series is discussed in [47, 72]. From a numerical point of view these equations can be solved to any desired finite order, resulting in an expansion which approximates the local manifold as well as we wish near the periodic orbit. In order to implement this scheme

we have to numerically solve this recursive system of equations in an efficient way. We would also like to have some indicators which describe how good our approximate solution is in a given fixed neighborhood of the periodic orbit.

In the present work we exploit the fact that an invertible change of coordinates, which we define in terms of the Floquet normal form, reduces each of the differential equations in the recursive scheme to constant coefficient. The transformed equations are solved in Fourier space, resulting in algebraic recurrence relations. Inverting the coordinate transformation gives us the desired coefficients for the parameterization. We also discuss a reliable and easy to implement a-posteriori error indicator which allows us to estimate the size of the domain on which our numerical solution provides a good approximation.

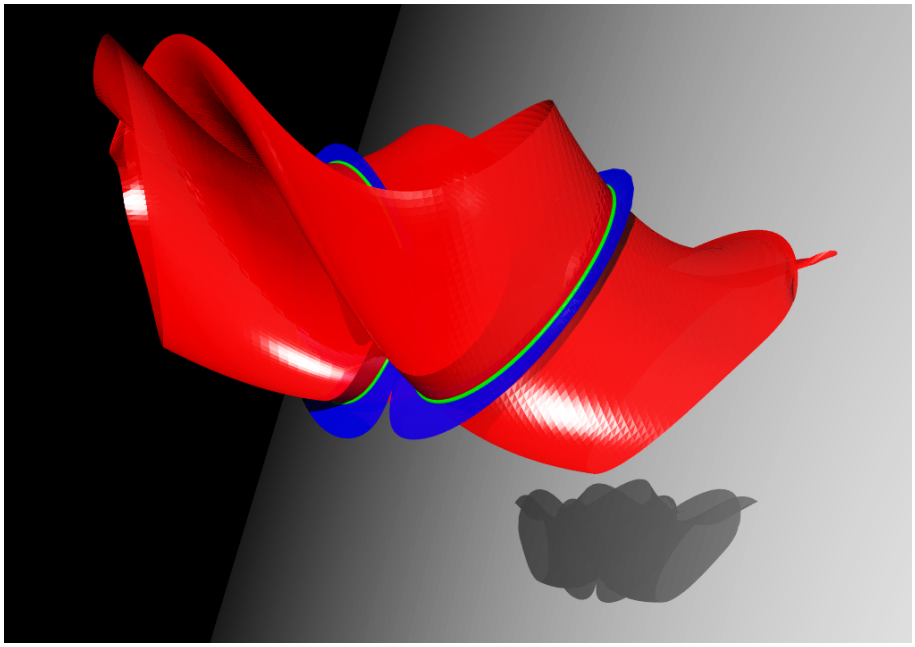

Figure 2: Local stable (red) and unstable (blue) manifolds associated with a hyperbolic periodic orbit (green) in the Lorenz attractor: again for the classical parameter values of $\rho = 28, \sigma = 10, \beta = 8/3$. This figure illustrates that the Parameterization Method provides expansions for the local invariant manifolds which are valid in rather large regions about the periodic orbit, and which expose nonlinear features of the manifolds. For example the local stable manifold shown here is roughly as wide as the global attractor itself. Both manifolds are parameterized by Fourier-Taylor expansions and no numerical integration has been employed in order to globalize the results.

Remark 1.1 (Numerical Computation of the Periodic Orbit and Its Floquet Normal Form)**.** We compute both the periodic orbit and its Floquet normal form using Fourier spectral methods. The numerically computed Fourier expansion for the orbit and the normal form are taken as the inputs for the invariant manifold computations. Spectral methods for numerically approximating periodic solutions of differential equations have a rich history, as can be seen by consulting almost any text on numerical analysis. We make no attempt to review the relevant literature on spectral methods. The interested reader can consult for

example [64, 48, 59, 71, 72, 80].

The approach used in the last two reference is especially relevant to the approach of the present work. In fact [80] develops a mathematically rigorous computer assisted method for bounding the error associated with spectral Fourier approximations of the Floquet normal form. These methods could be used in order to provide mathematically rigorous bounds on the initial data for the methods of the present work,

Remark 1.2 (Validated Numerics)**.** Combining the work of [80] with the techniques of the present work will lead to methods for obtaining mathematically rigorous bounds on the truncation error associated with our parameterization. See also the discussion in Section 5 of [47]. Once one has rigorous a-posteriori bounds on the Fourier-Taylor expansions of the local manifolds then it is possible to extend the methods of [63, 60, 61] in order to obtain computer assisted proof of transverse cycle-to-cycle and cycle-to-point connections for differential equations. Computer assisted validation for stable/unstable manifolds for periodic orbits is the topic of paper II.

The remainder of the paper is organized as follows. In Section 1.1 we provide some brief remarks on the literature. Section 2 comprises the mathematical core of the paper. Here we review the Floquet theory as well as the Parameterization Method. We derive the recursive system of differential equations for the Taylor coefficients of the stable/unstable manifold as eluded to above and solve the system via the Floquet form. Finally we discuss an a-posteriori error indicator for the method.

Section 3 deals with numerical computations. We begin with a detailed discussion of the computations illustrated in Figures 1 and 2. We also discuss the computation of some three dimensional stable manifolds for periodic orbits for three dimensional vector fields (these manifolds provide trapping regions, and generalize to three dimensions the work of [72]). Finally we discuss the computation of some invariant manifolds for a ten dimensional differential equation which arises as a truncation of the Kuramoto-Sivashinsky Partial Differential Equation.

The final section of the paper is Section 4 and we present some example computations where the parameterized manifolds are used in order to compute homoclinic connecting orbits via the method of projected boundaries. We look at some examples for the Lorenz system and also for a ten-dimensional Galerkin projection of the Kuramoto-Sivashinsky Equation.

1.1 Related Work

The literature on numerical computation of invariant objects for dynamical systems is vast and we attempt only a brief overview. Our primary objective is to direct the interested reader to more complete sources of information.

The central role to be played by invariant manifolds in the qualitative theory of dynamical systems is already anticipated in the work of Poincare. (See for example the historical discussion of this work found in Appendix B of [47]). By the mid 20-th Century results such as [52] made precise the fact that intersections of stable and unstable manifolds give rise to complicated dynamics. The advent of the computer as a tool for studying the dynamics of nonlinear systems led to much interest in numerical methods for computing invariant manifolds and their intersection, and by the mid 1980s there were already a number of researchers using the computer to study the intersections which Poincare remarked were difficult to draw. See the discussion in [37, 6, 7] and again the historical overview in [47].

Interest in the intersection of stable and unstable manifolds for applications has led to a great deal of work on numerical methods for globalizing local invariant manifolds. We refer the reader to the works of [25, 23, 22, 21, 20, 19, 42, 43] as well as to the review article [18]. The paper [24] treats the globalization of non-orientable stable/unstable manifolds of periodic orbits in differential equations, a subject which is also treated using the techniques of the present work. We also refer the reader to [23, 26, 27] for studies which investigate global information about a dynamical systems by studying the embedding of numerically globalized stable/unstable manifolds.

The region of phase space near an equilibria or periodic orbit can also be studied via the computation of normal forms, and by evaluating these normal forms on the stable or unstable subspaces one obtains numerical methods for computing stable and unstable manifolds. These computations can be made mathematically rigorous and play a critical role in the computer assisted proof of the existence of the Lorenz attractor [77, 78, 79]. See also [86] for an application of mathematically rigorous computation for invariant manifolds in celestial mechanics based on normal forms. Normal forms are also useful for computing invariant tori, and are used in the numerical study of many problems coming from celestial mechanics [28, 5, 38, 84, 85].

The Parameterization Method is a general functional analytic framework for studying invariant manifolds of nonlinear dynamical systems. The method was initially developed for studying stable/unstable manifolds associated with non-resonant fixed points of maps and equilibria of vector fields [45, 46, 47]. Chart maps computed using the parameterization have the additional property that they conjugate the dynamics on the invariant manifold to the dynamics of some well understood model system. Then the Parameterization Method provides insight into the dynamics on the manifold as well as information about the embedding.

The Parameterization Method has been extended in order to study invariant circles and invariant tori for diffeomorphisms and differential equations, and the method is also used to study stable/unstable manifolds of invariant circles [67, 68, 73, 74, 75]. More recently this work has been extended in order to simultaneously compute some invariant circles as well as to solve for the unknown conjugating dynamics [69, 70]. The Parameterization Method is also used in order to study some invariant manifolds associated with fixed points having some stable and some unstable directions [58].

Numerical methods for computing invariant manifolds based on the Parameterization method can be found in a number of works including [56, 57, 72, 42, 43, 82], along with the present work. A useful feature of methods based on Parameterization is that they admit natural a-posteriori error indicators. This notion can be used in order to obtain mathematically rigorous error bounds on the numerical approximation of the invariant manifolds by computer assisted analysis [63, 60, 61].

Another important application of the Parameterization Method is the development of KAM results which do not rely on the construction of action angle variables [66, 65]. There is also work which uses the Parameterization Method in order to devise KAM schemes for Volume preserving diffeomorphisms [83, 82]. The Parameterization Method has recently been used in order to develop KAM type theorems for dissipative systems [76] which are conformally symplectic.

One motivation for studying stable and unstable manifolds, as mentioned above, is the fact that their intersections give rise to orbits which connect different regions of phase space. Numerical methods for computing connecting orbits between many geometric objects are found for example in the work of [6, 7, 29, 31, 32, 34, 35, 36, 44, 49, 50]. Of course we refer to the works just cited for more thorough discussion of the literature. Connecting orbits

between invariant manifolds are exploited in many applications. Much work on studying transfer dynamics in celestial mechanics exploits these tools. See for example [2, 3, 4, 8, 9, 10, 11, 12, 33, 40, 41]. The study of invariant manifolds for periodic orbits also plays a role in the study of biological and chemical oscillations, and we refer for example to the work of [15, 13, 17, 16, 72]. The study of connecting orbits can be made mathematically rigorous using computer assisted proof, and we refer to [53, 54, 63, 61, 60] for more discussion of this theme.

Remark 1.3 (Computation of a Local Stable/Unstable Manifold Versus Globalization of a Local Stable/Unstable Manifold)**.** We remark that numerical methods based on the Parameterization Method, such as the methods developed in [56, 57, 72] and also in the present work, are methods for computing accurate local representations of the stable/unstable manifolds of invariant objects. In order to understand the global dynamics of a system it is natural to try to extend the local manifold via numerical integration.

This is a notoriously delicate problem as the flow induced by the vector field will stretch the boundary of the local manifold in highly nonlinear ways. For example simply numerically integrating points on the boundary of the unstable manifold for time $T > 0$ often yields unsatisfactory results, as the tendency is for the globalized object to grow much faster in some directions than in others. The numerical methods discussed in [18] provide techniques for globalizing local representations of stable/unstable manifolds in uniform ways.

An interesting line of research is to develop globalization schemes which apply globalization methods to the high order local manifold approximations given by the Parameterization method. The papers [42, 43] develop some techniques which show that this is a fruitful line of future inquiry. The Parameterization Method can be used to obtain differential geometric information (such as curvature) about stable/unstable manifolds away form the orbit, and also provides information about inflowing/outflowing properties the flow on the boundary of the local approximation. To the best of our knowledge no attempt has been made to develop globalization schemes which exploit this information, and this should be an interesting line of future study. Globalization of local invariant manifolds is not considered further in the present work.

2 The Parameterization Method for Invariant Manifolds of Periodic Orbits

In this section we review the Floquet theory and as much of the Parameterization Method as is used in the remainder of the present work. We also discuss the computation of the parameterization coefficients, the definition of the a-posteriori indicator function, and the effect the properties of the Floquet multipliers (such as sign, real versus complex conjugate, etc) have on the parameterization.

2.1 Review of the Real 2τ Periodic Floquet Normal Form of a Periodic Orbit

Given a periodic orbit the first order approximation of the stable invariant manifold is given by the stable normal bundle of the periodic orbit. The normal bundle is defined by solving the variational equation around the periodic orbit. To be more precise suppose $\gamma(t) : [0, \tau] \to \mathbb{R}^d$ is a τ-periodic orbit for the system $\dot{x} = f(x)$ and τ the minimal period. The variational equation is the system obtained by linearization of the vector field around

$\gamma(t)$, i.e.

$$\begin{cases} \dot{\Phi} = Df(\gamma(t))\Phi \\ \Phi(0) = I \end{cases} . \tag{1}$$

The solution $\Phi(\tau)$ of the above system after one period is called the *Monodromy* matrix of $\gamma(t)$ and it describes the stability of the periodic orbit. Indeed the number of eigenvalues of $\Phi(\tau)$ inside and outside the complex unit ball determines the dimension of the stable and unstable invariant manifolds while the eigenvectors associated to the eigenvalues determine the stable/unstable directions normal to the periodic orbit at the point $\gamma(0)$. Denote by E_s^0, E_u^0 the space spanned by the eigenvectors associated with the stable and unstable direction respectively. In order to have a complete bundle around the orbit, one should repeat the above procedure for any of the reparametrization $\gamma^\theta(t) = \gamma(t+\theta)$ yielding the monodromy matrices $\Phi^\theta(\tau)$ and the stable and unstable subspaces E_s^θ, E_u^θ in $\gamma(\theta)$. Thus one defines the normal bundles as

$$E_s = \bigcup_{\theta\in[0,\tau]} \gamma(\theta) \times E_s^\theta, \quad E_u = \bigcup_{\theta\in[0,T]} \gamma(\theta) \times E_u^\theta .$$

As mentioned above, the knowledge of the normal bundles is fundamental for the parametrization of the invariant manifold but the computation of E_s and E_u is not trivial. In terms of the stable/unstable manifold the essential point is that the normal bundles are the first order jets, i.e. the invariant manifolds are tangent to these linear bundles.

A classical method for computing the linear bundles is described for example in [14], and it is well known that it is enough to compute the tangent directions only once, for instance for $\theta = 0$, and then to use the Floquet normal form of the fundamental matrix solution of the variational system to compute the entire bundles. The real Floquet normal form decomposition of the solution $\Phi(t)$ of system (1), is a periodic matrix function $Q(t)$ that is to know to be a real 2τ-periodic and the real matrix R so that

$$\Phi(t) = Q(t)e^{Rt} .$$

The fundamental dynamical feature of the Floquet normal form is as follows: If $\{\phi_i\}_i$ denote the eigenvalues and $\{v_i\}_i$ the eigenvectors of $\Phi(\tau)$ then the eigenvector v_i^θ associated to the eigenvalue ϕ_i of the matrix $\Phi^\theta(\tau)$ are simply given by

$$w_i^\theta = Q(\theta)v_i.$$

In these terms the Floquet normal form of the solution $\Phi(t)$ allows us to have a complete parametrization of the stable and unstable normal bundles for γ. Note that the function $Q(t)$ is 2τ periodic thus the *dynamics* of the eigenvectors w_i^θ around the orbit γ is 2τ-periodic. Since the tangent bundle is clearly τ-periodic it means that $w_i^0 = \pm w_i^\tau$. In case 2τ is the minimal period for $Q(\theta)$ then $w_i^0 = -w_i^\tau$ and the bundle is said to have a twist. This occurs when the bundle is non-orientable.

Remark 2.1. Above we discussed about the real Floquet normal form, indeed it exists a different version, the complex Floquet normal form for the fundamental matrix solution $\Phi(t)$. According to the complex form, the function $\Phi(t)$ can be decomposed as $\Phi(t) = P(t)e^{Bt}$ for a possibly complex τ-periodic matrix function $P(t)$, $P(0) = I$ and constant matrix B. The eigenvalues μ_i of B are related to the eigenvalues λ_i of R by means of $(e^{\mu_i\tau})^2 = e^{\lambda_i 2\tau}$, where R is the matrix appearing in the real Floquet normal form. In particular, the real parts of μ_i and λ_i coincide. Moreover the matrix B and R have the same eigenvectors $\{v_i\}_i$ that are as well eigenvectors for $\Phi(\tau)$ and $\Phi(2\tau)$.

Remark 2.2 (Floquet Multipliers and Eigenvalues of the Poincare Map)**.** A classical fact is that the eigenvalues ϕ_i of $\Phi(\tau)$, also called the Floquet or characteristic multipliers, are the eigenvalues of the differential of the Poincare map at the fixed point. By definition, a Floquet exponent is any complex number μ_i such that $\phi_i = e^{\mu_i \tau}$. Hence, the eigenvalues of B, being B the exponent in the complex Floquet normal form, are Floquet exponents of the orbit γ. However, the eigenvalues λ_i of R, are related with ϕ_i by means of $\phi_i^2 = e^{2\lambda_i \tau}$. Note that λ_i alone is not enough to identify the Floquet multiplier ϕ_i, being $\phi_i = \pm e^{\lambda_i \tau}$. Nevertheless, the sign of the real part of λ_i determines the stability of the periodic orbit. For example the periodic orbit is hyperbolic if none of the multipliers lie on the unit circle or, equally, none of the exponents have zero real part. The number of multipliers inside the unit circle (number of exponents with negative real part) determines the number of stable directions of the orbit (similarly for the unstable directions).

Also, the sign of the real part of the Floquet multipliers tells us wether the orientation of the associated eigenvector is flipped by the Poincare map or not. If the real part is positive then the eigenvector is not flipped while real part negative implies the flip. For the periodic orbit this determines wether or not the linear bundle is orientable, i.e. If the orientation of the eigenvector is flipped then the linear bundle is a Mobius strip. The presence of complex conjugate multipliers implies that the dynamics in the linear bundle is rotational. Note that the presence of the twist can not be inferred from the eigenvalues of R, rather from the eigenvalues of B.

2.2 Invariance Equation

In this section we study an equation which characterizes chart maps for the local invariant stable/unstable manifold. The chart maps studied here have the additional property that they conjugate the dynamics on the manifold to a certain linear dynamical system. Throughout we discuss the stable manifold. The unstable manifold is obtained by reversing time.

Let $f(x) : \mathbb{R}^d \to \mathbb{R}^d$ be a real analytic vector field and suppose $\gamma(\theta)$ is a τ-periodic solution of $\dot{x} = f(x)$. Denote by $\mathbb{T}_{2\tau} = [0, 2\tau]_{/\{0,2\tau\}}$ the circle of length 2τ. Let ϕ: $\mathbb{R}^d \times \mathbb{R}^+ \to \mathbb{R}^d$ denote the flow generated by f. We assume without loss of generality that ϕ is globally well defined.

Suppose that $\gamma(\theta)$ is hyperbolic and let $\Phi(t) = Q(t)e^{Rt}$ be the real Floquet normal form of the fundamental matrix solution of the variational system. As in Section 1 we let $\lambda_1, \ldots, \lambda_{d_m} \in \mathbb{C}$ denote the stable eigenvalues of the matrix R and $w_1, \ldots, w_{d_m} : \mathbb{T}_{2\tau} \to \mathbb{R}^d$ denote the associated eigenvectors and assume that $w_1, \ldots, w_{d_m}$ are linearly independent over $\mathbb{T}_{2\tau}$.

With $\theta \in \mathbb{T}_{2\tau}$ and $\sigma \in \mathbb{R}^{d_m}$ we have that the stable normal bundle of γ is parameterized by

$$\mathbb{P}_1(\theta, \sigma) = \gamma(\theta) + \sum_{j=1}^{d_m} \xi_j(\theta)\sigma_j,$$

where

$$\xi_j(\theta) = Q(\theta)w_j,$$

i.e. $E_s = \text{image}\,(\mathbb{P}_1)$. One goal is to now find a nonlinear correction to $\mathbb{P}_1$ which results in a parameterization of the local stable manifold. In fact we obtain something stronger.

Suppose for the moment that the Floquet exponents are real and distinct with $\lambda_{d_m} < \ldots < \lambda_1 < 0$. (Other cases are similar and are discussed in Sections 2.8, and 2.9). We

consider the vector field

$$\dot{\theta} = 1, \quad \dot{\sigma} = \mathbf{\Lambda} \cdot \sigma, \qquad \mathbf{\Lambda} = \begin{pmatrix} \lambda_1 & & \\ & \ddots & \\ & & \lambda_{d_m} \end{pmatrix}. \tag{2}$$

Let

$$B_\nu = \left\{ \sigma \in \mathbb{R}^{d_m} \mid \max_{1 \le j \le d_m} |\sigma_j| \le \nu \right\}.$$

We refer to the cylinder $\mathbb{C}_{2\tau,\nu} \equiv \mathbb{T}_{2\tau} \times B_\nu$ as *the parameter space* for the local invariant manifold. Note that the $\sigma = 0$ set is an invariant circle for Equation (2). Also note that the vector field given by Equation (2) is inflowing on the parameter cylinder, i.e. for any $(\theta, \sigma) \in \partial\,\mathbb{C}_{2\tau,\nu}$ we have that the vector $(1, \Lambda\sigma)$ points inward toward the center of the cylinder. (This is the only place where we exploit that the eigenvalues are real distinct).

We have that the flow on the cylinder is given explicitly by the formula

$$\mathfrak{L}(\theta, \sigma, t) = \begin{bmatrix} \theta + t \\ e^{\Lambda t}\sigma \end{bmatrix}, \tag{3}$$

and this flow clearly maps $\mathbb{C}_{2\tau,\nu}$ into its own interior for any $t > 0$, with the circle $\sigma = 0$ a periodic orbit of period 2τ. We take the flow $\mathfrak{L}$ as the "model dynamics" on the stable manifold and look for a chart map which conjugates the nonlinear dynamics on $W^s_{\text{loc}}(\gamma)$ to the linear dynamics on $\mathbb{C}_{2\tau,\nu}$ given by $\mathfrak{L}$. More precisely we have the following definition.

Definition 2.3 (Conjugating Chart Map for the Local Stable Manifold)**.** We say that the function $\mathbb{P}\colon \mathbb{T}_{2\tau} \times B_r \to \mathbb{R}^d$ is a *conjugating chart map* for a local stable manifold of γ if

1. $\mathbb{P}$ is a continuous, surjective mapping of the cylinder $\mathbb{C}_{2\tau,\nu}$ which is real analytic on the interior of the cylinder.

2. $$\mathbb{P}(\theta, 0) = \gamma(\theta),$$

3. The conjugacy relation

$$\phi\left[\mathbb{P}(\theta, \sigma), t\right] = \mathbb{P}\left(\theta + t, e^{\Lambda t}\sigma\right), \tag{4}$$

   is satisfied for all $\theta \in \mathbb{T}_{2\tau}$, $\sigma \in B_\nu$, and $t \ge 0$.

The definition asks that P conjugates the flow generated by the vector field f to the linear flow generated by Equation (3). Note that if $\mathbb{P}$ is a conjugating chart map then for any $(\theta, \sigma) \in \mathbb{C}_{2\tau,\nu}$ we have that

$$\begin{aligned} \lim_{t\to\infty} \|\phi[\mathbb{P}(\theta,\sigma), t] - \gamma(\theta + t)\| &= \lim_{t\to\infty} \left\|\mathbb{P}\left(\theta + t, e^{\Lambda t}\sigma\right) - \gamma(\theta + t)\right\| \\ &= \lim_{t\to\infty} \|\mathbb{P}\left(\theta + t, 0\right) - \gamma(\theta + t)\| \\ &= 0 \end{aligned} \tag{5}$$

by the continuity of $\mathbb{P}$, the conjugacy relation (4) and the contractiveness of $e^{\Lambda t}$. This says that the orbit of a point in the image of $\mathbb{P}$ accumulates to the periodic orbit γ with matching asymptotic phase θ. In addition, since $\mathbb{P}$ is one-to-one it's image is a d_m dimensional manifold (immersed disk). Since image($\mathbb{P}$) is an immersed disk containing γ in its interior

and having that each of its points accumulates on γ under the forward flow, image($\mathbb{P}$) is a local stable manifold for γ.

The following Theorem provides sufficient conditions for the existence of a conjugating chart map.

Theorem 2.4 (Invariance Equation for a Conjugating Chart Map)**.** *Suppose that* $\mathbb{P}\colon \mathbb{T}_{2\tau} \times B_\nu \to \mathbb{R}^d$ *is a continuous function having that*

$$\mathbb{P}(\theta, 0) = \gamma(\theta) \qquad \text{for all } \ \theta \in \mathbb{T}_{2\tau}, \tag{6}$$

that $\mathbb{P}$ *is differentiable on the circle* $\sigma = 0$ *with*

$$\frac{\partial}{\partial \sigma_j}\mathbb{P}(\theta, 0) = w_j(\theta) \qquad \text{for each } \ 1 \le j \le d_m, \tag{7}$$

and that $\mathbb{P}(\theta, \sigma)$ *solves the partial differential equation*

$$\frac{\partial}{\partial \theta}\mathbb{P}(\theta, \sigma) + \sum_{i=1}^{d_m} \lambda_i \sigma_i \frac{\partial}{\partial \sigma_i}\mathbb{P}(\theta, \sigma) = f(\mathbb{P}(\theta, \sigma)), \tag{8}$$

on the interior of $\mathbb{C}_{2\tau,\nu}$*. Then* $\mathbb{P}$ *is a conjugating chart map for* γ *in the sense of Definition 2.3. It follows from Equation (5) that image*($\mathbb{P}$) *is a local stable manifold for* γ*.*

Proof. To see that $\mathbb{P}$ is a conjugating chart map choose $(\theta_0, \sigma_0) \in \mathbb{C}_{2\tau,\nu}$ and define the curve $x\colon [0, \infty) \to \mathbb{R}^d$ by

$$x(t) = \mathbb{P}(\theta_0 + t, e^{\Lambda t}\sigma_0) = \mathbb{P}(\mathfrak{L}(\theta, \sigma, t)).$$

We begin by noting that $x(t) \in$ image($\mathbb{P}$) for all $t \ge 0$, as $\mathfrak{L}$ is contracting on $\mathbb{C}_{2\tau,\nu}$. Next we show that $x(t)$ solves the initial value problem

$$x'(t) = f[x(t)] \qquad x(0) = \mathbb{P}(\theta_0, \sigma_0), \tag{9}$$

in forward time. To see this note that

$$\begin{aligned} x'(t) &= \frac{d}{dt}\mathbb{P}(\theta_0 + t, e^{\Lambda t}\sigma_0) \\ &= D_{\theta,\sigma}\mathbb{P}(\theta_0 + t, e^{\Lambda t}\sigma_0) \begin{bmatrix} 1 \\ e^{\Lambda t}\Lambda\sigma_0 \end{bmatrix} \\ &= \frac{\partial}{\partial \theta}\mathbb{P}(\theta_0 + t, e^{\Lambda t}\sigma_0) + \sum_{j=1}^{d_m} \mathbb{P}(\theta_0 + t, e^{\Lambda t}\sigma_0)\lambda_j e^{\lambda_j}\sigma_j^0. \end{aligned}$$

Now define the new variables $\hat{\sigma}_j = e^{\lambda_j t}\sigma_j^0$ for $1 \le j \le d_m$ and $\hat{\theta} = (\theta_0 + t)_{\mathrm{mod} 2\tau}$. Then for any $t > 0$ we have that $(\hat{\theta}, \hat{\sigma}) \in$ interior $(\mathbb{C}_{2\tau,\nu})$. Since Equation (8) holds on the interior by hypothesis we now have that

$$\begin{aligned} \frac{\partial}{\partial \theta}\mathbb{P}(\theta_0 + t, e^{\Lambda t}\sigma_0) + \sum_{j=1}^{d_m} \mathbb{P}(\theta_0 + t, e^{\Lambda t}\sigma_0)\lambda_j e^{\lambda_j}\sigma_j^0 &= \frac{\partial}{\partial \theta}\mathbb{P}(\hat{\theta}, \hat{\sigma}) + \sum_{j=1}^{d_m} \mathbb{P}(\hat{\theta}, \hat{\sigma})\lambda_j \hat{\sigma}_j \\ &= f\left[\mathbb{P}(\hat{\theta}, \hat{\sigma})\right]. \end{aligned}$$

But $\mathbb{P}(\hat{\theta}, \hat{\sigma}) = x(t)$, so this shows that

$$x'(t) = f\left[x(t)\right],$$

for all $t > 0$ as desired. Since $x(0) = P(\theta_0, \sigma_0)$ by definition we indeed have that $P(\theta_0 + t, e^{\Lambda t}\sigma_0)$ solves Equation (9). But (θ_0, σ_0) was arbitrary in $\mathbb{C}_{2\tau,\nu}$, so this shows that

$$x(t) = \mathbb{P}(\theta + t, e^{\Lambda t}\sigma) = \phi\left[\mathbb{P}(\theta, \sigma), t\right],$$

and $\mathbb{P}$ satisfies Equation 4 on $\mathbb{C}_{2\tau,\nu}$.

Then $\mathbb{P}$ satisfies condition (3) of Definition (2.3). We now establish (1) and (2) of the same. First note that since f is real analytic and $\mathbb{P}$ solves the differential Equation (8), we have that $\mathbb{P}$ is is real analytic in the interior of $\mathbb{C}_{2\tau,\nu}$. From Equation (7) we have that

$$D_\sigma \mathbb{P}(\theta, 0) = [w_1(\theta)| \dots |w_{d_m}(\theta)].$$

Since the eigenvectors are linearly independent over $\mathbb{T}_{2\tau}$ we have that $D_\sigma \mathbb{P}(\theta, 0)$ is full rank. Since $\mathbb{P}$ is real analytic it is certainly continuously differentiable, and the continuity of the derivative implies that the differential is full rank in a neighborhood of γ, i.e. there is an $r > 0$ so that $\|\sigma\| \leq r$ implies that $D_\sigma \mathbb{P}(\theta, \sigma)$ is full rank. If follows from the implicit function theorem that $\mathbb{P}$ is injective for $\|\sigma\| < r$.

Then consider $(\theta_1, \sigma_1), (\theta_2, \sigma_2) \in \mathbb{C}_{2\tau,\nu}$ and suppose that

$$\mathbb{P}(\theta_1, \sigma_1) = \mathbb{P}(\theta_2, \sigma_2). \tag{10}$$

Since $e^{\Lambda t} \to 0$ as $t \to \infty$ there is a $\hat{t}$ so large that

$$\left\| e^{\Lambda \hat{t}}\sigma_1 \right\|, \left\| e^{\Lambda \hat{t}}\sigma_2 \right\| < r. \tag{11}$$

Since $\mathbb{P}$ satisfies the conjugacy Equation (4) we have that

$$\mathbb{P}\left(\theta_1 + \hat{t}, e^{\Lambda \hat{t}}\sigma_1\right) = \phi\left[\mathbb{P}(\theta_1, \sigma_1), \hat{t}\right], \quad \text{and} \quad \mathbb{P}\left(\theta_2 + \hat{t}, e^{\Lambda \hat{t}}\sigma_2\right) = \phi\left[\mathbb{P}(\theta_2, \sigma_2), \hat{t}\right].$$

From Equation (10) (as well as the uniqueness of trajectories under ϕ) it follows that

$$\mathbb{P}\left(\theta_1 + \hat{t}, e^{\Lambda \hat{t}}\sigma_1\right) = \mathbb{P}\left(\theta_2 + \hat{t}, e^{\Lambda \hat{t}}\sigma_2\right)$$

But now it follows from the conditions of (11) that

$$\left(\theta_1 + \hat{t}, e^{\Lambda \hat{t}}\sigma_1\right) = \left(\theta_2 + \hat{t}, e^{\Lambda \hat{t}}\sigma_2\right),$$

as $\mathbb{P}$ is injective on $\mathbb{T}_{2\tau} \times B_r$. Since the linear flow map is invertible at $\hat{t}$ we have that $(\theta_1, \sigma_1) = (\theta_2, \sigma_2)$ hence $\mathbb{P}$ is an injection of $\mathbb{C}_{2\tau,\nu}$ into $\mathbb{R}^d$. Then $\mathbb{P}$ is a conjugating chart map for the stable manifold of γ as desired. □

Remark 2.5 (Converse of Lemma 2.4)**.** It is not difficult to see that the converse of the Theorem holds. Indeed if $\mathbb{P}$ satisfies (6), (7), and in addition is a differentiable conjugating chart map in the sense of Definition 4, then $\mathbb{P}$ is a solution of the partial differential equation (8). To see this one differentiates the conjugacy Equation (4) with respect to time, and takes the limit as $t \to 0$ in the resulting expression to recover Equation (8). Then Equation (8) subject to the first order constraints (6) and (7) constitute necessary and sufficient conditions for the existence of a conjugating chart map parameterizing a local stable manifold for γ. The length of the eigenvectors is unspecified throughout this discussion, and it follows that the conjugating chart map $\mathbb{P}$ is unique up to the choice of this scaling.

The preceding discussion shows that in order to study the local invariant manifold of γ it is enough to study Equation (8), appropriately constrained. The following provides a necessary condition for the existence of solutions of Equation (8), in terms of certain algebraic constraints between the stable eigenvalues.

Definition 2.6 (Resonant Eigenvalues)**.** We say that the stable eigenvalues $\lambda_1, \ldots, \lambda_{d_m}$ are resonant at order $\alpha \in \mathbb{N}^{d_m}$ if there is a $1 \leq j \leq d_m$ so that

$$\alpha_1\lambda_1 + \ldots + \alpha_{d_m}\lambda_{d_m} - \lambda_j = 0. \tag{12}$$

Lemma 2.7 (Divergence Theorem)**.** If there is a resonance in the sense of Definition 2.6 at some order $|\alpha| \geq 2$ then Equation (8) has no solution.

The proof follows from the computations in Section 2.4. In particular see Remark 2.11 and also [47]

So, Lemma 2.7 provides conditions under which we fail to have solutions of the invariance equation. Also observe that there can be no resonances of order $\alpha \in \mathbb{N}^{d_m}$ when

$$2 \leq |\alpha| \leq \left\lceil \frac{\text{real}(\lambda_1)}{\text{real}(\lambda_{d_m})} \right\rceil,$$

i.e. α is eventually large enough that (12) cannot hold as the $\lambda_1, \ldots, \lambda_{d_m}$ have the same sign. Then in fact there are only a finite number of possible resonances, and this finite number is determined by the so called "spectral gap" (ratio of the largest and smallest real part taken over the set of stable eigenvalues). For a more thorough discussion of resonances see [45, 46, 47, 60, 63].

2.3 Homological equations

In this section we develop a formal series solution for Equation (8). Explicitly we assume a series solution of the form

$$\mathbb{P}(\theta, \sigma) = \sum_{|\alpha|=0}^{\infty} a_\alpha(\theta)\sigma^\alpha = \sum_{|\alpha|=0}^{\infty} \sum_{k\in\mathbb{Z}} a_{\alpha,k} e^{\frac{2\pi i}{2\tau}k\theta}\sigma^\alpha. \tag{13}$$

Here $\alpha \in \mathbb{N}^{d_m}$ is a d_m-dimensional multi-index, $a_{\alpha,k} \in \mathbb{R}^d$ for all α and k. We refer to an exapnsion of the form given by Equation (13) as a *Fourier-Taylor series*. We substitute (13) into the invariance equation (8) and we expand the vector field $f(\mathbb{P}(\theta, \sigma))$ as its Taylor series with respect to the variable σ centered in $\sigma = 0$, i.e.

$$f(\mathbb{P}(\theta,\sigma)) = f(\mathbb{P}(\theta,0)) + \sum_{i=1}^{d_m} \frac{\partial}{\partial\sigma_i} f(\mathbb{P}(\theta,0))\sigma_i + \sum_{|\alpha|\geq 2} \frac{1}{\alpha!} f^{(\alpha)}(\mathbb{P}(\theta,0))\sigma^\alpha$$

where $f^{(\alpha)}(\mathbb{P}(\theta,0))$ is the derivative $\frac{\partial^{|\alpha|}}{\partial\sigma^\alpha} f(\mathbb{P}(\theta,\sigma))$ evaluated in $\sigma = 0$. Then we collect the terms with the same power of σ and we solve the resulting equations. Since

$$\frac{\partial}{\partial\theta}\mathbb{P}(\theta,\sigma) = \sum_{|\alpha|\geq 0} \Big(\frac{d}{d\theta} a_\alpha(\theta)\Big)\sigma^\alpha, \qquad \frac{\partial}{\partial\sigma_i}\mathbb{P}(\theta,\sigma) = \sum_{|\alpha|>0} a_\alpha \alpha_i \sigma^\alpha \sigma_i^{-1}$$

we end up with the following sequence of differential equations.

$|\alpha| = 0$: The only multi-index with zero length is $\mathbf{0} = (0, \dots, 0)$. The terms in $\sigma^{\mathbf{0}}$ give

$$\frac{d}{d\theta} a_{\mathbf{0}}(\theta) = f(a_{\mathbf{0}}(\theta))$$

whose solution is given by the periodic orbits itself, hence $a_{\mathbf{0}}(\theta) = \gamma(\theta)$.

$|\alpha| = 1$: The multi-indices of length 1 are $e_i = (0, \dots, 1, \dots, 0)$ with 1 in the i-th position. Since $\frac{\partial}{\partial \sigma_i} f(\mathbb{P}(\theta, 0))\sigma_i = Df(a_{\mathbf{0}}(\theta))a_{e_i}(\theta)$, equating the terms in σ^{e_i} we end up with

$$\begin{cases} \frac{d}{d\theta} a_{e_i}(\theta) + \lambda_i a_{e_i}(\theta) = Df(a_{\mathbf{0}}(\theta))a_{e_i}(\theta) \\ \\ \lambda_i \in \mathbb{R},\ a_{e_i}(\theta)\ 2\tau-\text{periodic} \end{cases} \qquad \forall i = 1, \dots, d_m. \tag{14}$$

$|\alpha| \geq 2$: It is easy to see that, once $a_{\mathbf{0}}(\theta)$ and $a_{e_i}(\theta)$ are given, we obtain equations of the form

$$\frac{da_\alpha(\theta)}{d\theta} + \alpha \cdot \boldsymbol{\lambda} a_\alpha(\theta) = Df(a_{\mathbf{0}}(\theta))a_\alpha(\theta) + \boldsymbol{R}_\alpha(\theta), \tag{15}$$

where $\boldsymbol{R}_\alpha$ involves only lower order terms. Equation (15) is referred to as the **homological equation** for the coefficient $a_\alpha(\theta)$. In case the non linearity of $f(x)$ is polynomial, the computation of the remaining terms $\boldsymbol{R}_\alpha$ can be done easily by means of the Cauchy products. Indeed the polynomials coincide with the Taylor polynomial.

We prove that all the solutions of (14) are $(\lambda_i, a_{e_i}(\theta)) = (\lambda_i, Q(\theta)v_i)$ where (λ_i, v_i) is any eigenpair of the matrix R appearing in the Floquet decomposition.

Proposition 2.8. *Let $\Phi(t) = Q(t)e^{Rt}$ be the real Floquet normal form decomposition of the fundamental matrix solution of system* (1)*. Then all the solutions $(\lambda_i, a_{e_i}(\theta))$ of* (14) *are given by $(\lambda_i, Q(\theta)\xi_i)$ with $(\lambda_i, \xi_i) \in \Sigma(R)$.*

Proof. For any λ, the function $\Phi_\lambda(\theta) = \Phi(\theta)e^{-\lambda\theta}$ is the fundamental matrix solution of $\dot{x} = Df(\gamma(t))x - \lambda x$. Indeed

$$\dot{\Phi}_\lambda(\theta) = \dot{\Phi}e^{-\lambda\theta} - \lambda\Phi(\theta)e^{-\lambda\theta} = Df(\gamma)\Phi(\theta)e^{-\lambda\theta} - \lambda\Phi(\theta)e^{-\lambda\theta} = Df(\gamma)\Phi_\lambda(\theta) - \lambda\Phi_\lambda(\theta)$$

and $\Phi_\lambda(0) = Id$. Let $(\lambda_i, \xi_i) \in \Sigma(R)$ and define $a_{e_i}(\theta) = \Phi_{\lambda_i}(\theta)\xi_i$. Thus $(\lambda_i, a_{e_i}(\theta))$ is a solution of Equation (14). Moreover, since (λ_i, ξ_i) is an eigenpair of R, it follows that

$$a_{e_i}(\theta) = \Phi(\theta)e^{-\lambda_i\theta}\xi_i = e^{-\lambda_i\theta}Q(\theta)e^{R\theta}\xi_i = e^{-\lambda_i\theta}Q(\theta)e^{\lambda_i\theta}\xi_i = Q(\theta)\xi_i$$

proving that $a_{e_i}(\theta)$ is 2τ-periodic. We conclude that $(\lambda_i, Q(\theta)\xi_i)$ is a solution of (14).

On the contrary, suppose $(\lambda_i, a_{e_i}(\theta))$ is a solution of problem (14). Thus

$$a_{e_i}(\theta) = \Phi_{\lambda_i}(\theta)a_{e_i}(0) = \Phi(\theta)e^{-\lambda_i\theta}a_{e_i}(0).$$

Being $a_{e_i}(\theta)$ 2τ-periodic, it follows that $a_{e_i}(0) = a_{e_i}(2\tau) = \Phi(2\tau)e^{-\lambda_i 2\tau}a_{e_i}(0)$, that is $(e^{2\lambda_i\tau}, a_{e_i}(0)) \in \Sigma(\Phi(2\tau))$. From the normal form decomposition we have that $\Phi(2\tau) = e^{2\tau R}$ and that the spectrum of R is in one-to-one correspondence with the spectrum of $\Phi(2\tau)$ so that $(\lambda, v) \in \Sigma(R)$ if and only if $(e^{2\tau\lambda}, \xi) \in \Sigma(\Phi(2\tau))$. We conclude that $a_{e_i}(0) = \xi_i$ and $(\lambda_i, \xi_i) \in \Sigma(R)$. From this it follows that $a_{e_i}(\theta) = Q(\theta)\xi_i$.

□

The existence of 2τ-periodic solutions of (15) is discussed in the following theorem.

Theorem 2.9. *If $e^{2\mu\tau}$ is not an eigenvalue of $\Phi(2\tau)$ then, for any 2τ-periodic function $\boldsymbol{R}_\alpha$, there exists a 2τ-periodic solution of $(\frac{d}{d\theta} - Df(a_{\mathbf{0}}) + \mu)a_\alpha = \boldsymbol{R}_\alpha$.*

Proof. See [47]. □

Taking $\mu = \alpha \cdot \boldsymbol{\lambda}$, if $e^{2\alpha\cdot\boldsymbol{\lambda}\tau}$ is not an eigenvalue of $\Phi(2\tau)$, there exist 2τ-periodic functions $a_\alpha(\theta)$ solutions of (15). That comes from the previous theorem and from the fact that the remaining term $\boldsymbol{R}_\alpha$ is 2τ-periodic.

2.4 Efficient solution of the homological equations: reducibility via the Floquet normal form

The situation encountered in Section 2.3, namely where one is trying to solve an invariance equation for a conjugating map and finds that the problem reduces to solving infinitely many linear equations, is a not uncommon. It arises frequently in the study of normal forms and we refer again to the treatment in [37] and [77]. As often happens in normal form theory we find that solving the resulting system of infinitely many linear differential equations is nontrivial, and seek further reduction.

For example when studying conjugating maps and normal forms for invariant objects in Hamiltonian dynamical systems it is sometimes possible to exploit the preservation of geometric structure in order to obtain a change of coordinates which reduces the homological equations to constant coefficient (or perhaps to constant coefficient plus a quadratically small error). We refer to [65] for a much more complete elaboration on this theme. The interested reader can also refer to [66] for a discussion of computing invariant tori in Hamiltonian systems without the use of action angle variables. CITE TIM and JIM use these ideas to compute invariant tori in volume preserving systems. See [58] for an example involving invariant manifolds for fixed points having some stable and some unstable directions in both symplectic and volume preserving systems. Another recent advance in this direction has been the extension of KAM theory to certain dissipative systems which preserve a conformally symplectic structure [76].

The point of these examples is that the choice of an appropriate coordinate system greatly simplifies the study and computation of invariant objects in dynamical systems theory. In this section we observe that reducibility for the problem of parameterizing the stable/unstable manifold of a non-resonant hyperbolic periodic orbit is achieved using a coordinate change given by the Floquet normal form. In fact we will see that the homological equations (15) are reduced to *diagonal constant coefficient in Fourier space*, and this in fact leads to particularly simple equations for the Fourier-Taylor coefficients for the desired conjugating chart map. The interested reader may contrast this to the approach of [72] where the homological equations (15) are solved for planar systems without using the Floquet normal form.

In order to formalize this discussion recall that Q is a solution of the differential equation

$$Q'(\theta) + Q(\theta)R = Df[\gamma(\theta)]Q(\theta) \tag{16}$$

with R a real-valued matrix. We assume that R is diagonalizable with

$$R = M\Sigma M^{-1},$$

and that

$$\Sigma = \begin{pmatrix} \Lambda_s & 0 & 0 \\ 0 & \Lambda_u & 0 \\ 0 & 0 & 0 \end{pmatrix}.$$

Here Λ_s is the $d_m \times d_m$ diagonal matrix of eigenvalues with negative real parts and Λ_u is the diagonal matrix of eigenvalues with positive real parts. As before $v_1, \ldots, v_{d_m}$ are the eigenvectors associated with the stable eigenvalues. Since R is diagonalizable the v_j, $1 \leq j \leq d_m$ are linearly independent. Again the functions $w_j(\theta) = Q(\theta)v_j$ parameterize the stable invariant vector bundle.

We will now see that the homological equation (15) is reduced to constant coefficient by the Floquet normal form. For $|\alpha| \geq 2$ define the functions $w_\alpha(\theta) : \mathbb{T}_{2\tau} \to \mathbb{R}^d$ by the coordinate transformation

$$a_\alpha(\theta) = Q(\theta)w_\alpha(\theta).$$

Taking into account (16), the equation (15) is transformed into the constant coefficient ordinary differential equation

$$\frac{d}{d\theta}w_\alpha(\theta) + ((\alpha_1\lambda_1 + \ldots + \alpha_{d_m}\lambda_{d_m})\mathrm{Id} - R)\, w_\alpha(\theta) = Q^{-1}(\theta)\boldsymbol{R}_\alpha(\theta). \tag{17}$$

We now let

$$w_\alpha(\theta) = \sum_{k\in\mathbb{Z}} (w_\alpha)_k e^{\frac{2\pi i k}{2\tau}\theta}$$

and

$$Q^{-1}(\theta)\boldsymbol{R}_\alpha(\theta) = \sum_{k\in\mathbb{Z}} (A_\alpha)_k e^{\frac{2\pi i k}{2\tau}\theta}.$$

$(w_\alpha)_k, (A_\alpha)_k \in \mathbb{C}^d$. We make a final coordinate transformation and define

$$(w_\alpha)_k = M(v_\alpha)_k.$$

Then Equation (17) gives

$$(v_\alpha)_k = \left[\left(\frac{2\pi i k}{2\tau} + \alpha_1\lambda_1 + \ \ldots + \alpha_{d_m}\lambda_{d_m}\right)\mathrm{Id} - \Sigma\right]^{-1} M^{-1}(A_\alpha)_k.$$

But this is diagonalized and solving component-wise we obtain

$$(v_\alpha)_k^{(j)} = \frac{1}{\frac{2\pi i k}{2\tau} + \alpha_1\lambda_1 + \ldots + \alpha_{d_m}\lambda_{d_m} - \lambda_j}(M^{-1}(A_\alpha)_k)^{(j)}, \tag{18}$$

for $1 \leq j \leq d_m$. Working backward from $v_\alpha(\theta)$ we obtain the desired solution $a_\alpha(\theta)$ by

$$a_\alpha(\theta) = Q(\theta)Mv_\alpha(\theta). \tag{19}$$

Remark 2.10 (Efficient Numerical Computations)**.** If the Fourier coefficients for both the periodic orbit $\gamma(\theta)$ and it's Floquet normal form $Q(\theta)$ are known, then the recurrence equations given in (18) combined with the coordinate transformation given by Equation (19) provide a recipe for computing the conjugating chart map $\mathbb{P}(\theta, \sigma)$ to any desired finite order. This is how we obtain the numerical approximations used in Sections 3 and 4. The reader interested in the numerical implementation can refer to our MatLab codes, which are available at (CITE WEB PAGE).

Of course this also assumes that that form of the functions $\boldsymbol{R}_\alpha(\theta)$ are known explicitly. In Section 2.5 we illustrate this computation for the Lorenz system. The computations are similar for the other examples considered and the present work and again the interested reader can view the numerical implementations for more details (CITE WEB PAGE).

Remark 2.11 (Resonances Revisited)**.** The Fourier-Taylor coefficients $(v_\alpha)_k^{(j)}$ defined by Equation (18) are formally well defined to all orders precisely when there are no resonances in the sense of Definition 2.6. This fact establishes Lemma 2.7.

2.5 Explicit Solution of the Homological Equations in an Example Problem: Periodic Orbits in the Lorenz System

The full computation of the homological equations, including the derivation of the precise form of the right-hand-sides $\boldsymbol{R}_\alpha(\theta)$ is best illustrated in the context of specific examples. To this end, recall that the Lorenz equations is given by the quadratic vector field

$$f(x,y,z) = \begin{pmatrix} -sx + sy \\ \rho x - y - xz \\ -\beta z + xy \end{pmatrix}, \tag{20}$$

where s, β, and ρ are parameters. We now expand the τ-periodic solution γ by considering it as a 2τ-periodic function, that is

$$\gamma(\theta) = \sum_{k\in\mathbb{Z}} \gamma_k e^{\frac{2\pi i k}{2\tau}\theta}.$$

Let

$$Q(\theta) = \sum_{k\in\mathbb{Z}} Q_k e^{\frac{2\pi i k}{2\tau}\theta}$$

be the Fourier expansion of the 2τ-periodic Floquet normal form of $\Phi(t)$ and chose $(\lambda,\xi) \in \Sigma(R)$, $\lambda \neq 0$.

We seek a function

$$\mathbb{P}(\theta,\sigma) = \sum_{\alpha=0}^{\infty} a_\alpha(\theta)\sigma^\alpha = \sum_{\alpha=0}^{\infty}\sum_{k\in\mathbb{Z}} (a_\alpha)_k e^{\frac{2\pi i k}{2\tau}\theta}\sigma^n, \tag{21}$$

solving Equation (1). Denote $a_\alpha = (a_\alpha^{(1)}, a_\alpha^{(2)}, a_\alpha^{(3)})^T \in \mathbb{R}^3$. Then we require that $\mathbb{P}(\theta,0) = \gamma(\theta)$ and $\frac{\partial}{\partial\theta}\mathbb{P}(\theta,0) = \xi(\theta)$ and take

$$(a_0)_k = \gamma_k \qquad \text{and} \qquad (a_1)_k = Q_k\xi,$$

for all $k \in \mathbb{Z}$. This determines the parameterization to first order. In order to determine the higher order coefficients we plug the unknown expansion given by Equation (21) into the invariance equation (8) and obtain

$$\frac{\partial}{\partial\theta}\mathbb{P}(\theta,\sigma) + \lambda\sigma\frac{\partial}{\partial\sigma}\mathbb{P}(\theta,\sigma) = \begin{pmatrix} -s\mathbb{P}_1(\theta,\sigma) + s\mathbb{P}_2(\theta,\sigma) \\ \rho\mathbb{P}_1(\theta,\sigma) - \mathbb{P}_2(\theta,\sigma) - (\mathbb{P}_1\cdot\mathbb{P}_3)(\theta,\sigma) \\ -\beta\mathbb{P}_3(\theta,\sigma) + (\mathbb{P}_1\cdot\mathbb{P}_2)(\theta,\sigma) \end{pmatrix}, \tag{22}$$

where

$$(\mathbb{P}_1\cdot\mathbb{P}_2)(\theta,\sigma) = \sum_{\alpha=0}^{\infty} p_\alpha^{(1,2)}(\theta)\sigma^\alpha \quad \text{and} \quad (\mathbb{P}_1\cdot\mathbb{P}_3)(\theta,\sigma) = \sum_{\alpha=0}^{\infty} p_\alpha^{(1,3)}(\theta)\sigma^\alpha,$$

with

$$p_\alpha^{(1,2)}(\theta) \stackrel{\text{def}}{=} \sum_{\substack{\alpha_1+\alpha_2=\alpha \\ \alpha_i\geq 0}}^{\infty} a_{\alpha_1}^{(1)}(\theta)a_{\alpha_2}^{(2)}(\theta) \quad \text{and} \quad p_\alpha^{(1,3)}(\theta) \stackrel{\text{def}}{=} \sum_{\substack{\alpha_1+\alpha_2=\alpha \\ \alpha_i\geq 0}}^{\infty} a_{\alpha_1}^{(1)}(\theta)a_{\alpha_2}^{(3)}(\theta).$$

It is convenient to separate in $p_\alpha^{(i,j)}$ the highest (in α) order terms

$$p_\alpha^{(1,2)}(\theta) = a_\alpha^{(1)}(\theta)a_0^{(2)}(\theta) + a_0^{(1)}(\theta)a_\alpha^{(2)}(\theta) + \tilde{p}_\alpha^{(1,2)}(\theta),$$

$$p_\alpha^{(1,3)}(\theta) = a_\alpha^{(1)}(\theta)a_0^{(3)}(\theta) + a_0^{(1)}(\theta)a_\alpha^{(3)}(\theta) + \tilde{p}_\alpha^{(1,3)}(\theta)$$

with

$$\tilde{p}_\alpha^{(1,2)}(\theta) \stackrel{\text{def}}{=} \sum_{\substack{\alpha_1+\alpha_2=\alpha \\ \alpha_i>0}}^{\infty} a_{\alpha_1}^{(1)}(\theta)a_{\alpha_2}^{(2)}(\theta) \quad \text{and} \quad \tilde{p}_\alpha^{(1,3)}(\theta) \stackrel{\text{def}}{=} \sum_{\substack{\alpha_1+\alpha_2=\alpha \\ \alpha_i>0}}^{\infty} a_{\alpha_1}^{(1)}(\theta)a_{\alpha_2}^{(3)}(\theta).$$

The reason of the last definition stands on the fact that, when matching like powers of σ in the right term of (22), the coefficient of σ^α is given by

$$\begin{pmatrix} -sa_\alpha^{(1)} + sa_\alpha^{(2)} \\ \rho a_\alpha^{(1)} - a_\alpha^{(2)} - p_\alpha^{(1,3)} \\ -\beta a_\alpha^{(3)} + p_\alpha^{(1,2)} \end{pmatrix} = Df(a_0)a_\alpha + \begin{pmatrix} 0 \\ -\tilde{p}_\alpha^{(1,3)}(\theta) \\ \tilde{p}_\alpha^{(1,2)}(\theta) \end{pmatrix}.$$

Therefore, matching the coefficients of σ^α in (22), it descends that the functions $a_\alpha(\theta)$ satisfy the differential equations

$$\frac{d}{d\theta}a_\alpha(\theta) + \lambda\alpha a_\alpha(\theta) - Df[\gamma(\theta)]a_\alpha(\theta) = \boldsymbol{R}_\alpha(\theta) \tag{23}$$

where the function $\boldsymbol{R}_\alpha(\theta)$ is defined recursively by the expression

$$\boldsymbol{R}_\alpha(\theta) = \begin{pmatrix} 0 \\ -\tilde{p}_\alpha^{(1,3)}(\theta) \\ \tilde{p}_\alpha^{(1,2)}(\theta) \end{pmatrix}$$

which involves only lower order terms. Here we have used the fact that $a_0(\theta) = \gamma(\theta)$ as well as the analytic expression for $Df(x, y, z)$. Equation (23) is referred to as the *homological equation* for the coefficients of $\mathbb{P}$. Now that $\boldsymbol{R}_\alpha(\theta)$ is known, the parameterization coefficients are computed directly using Equation (18).

Remark 2.12 (Non-Resonance and Numerics for Lorenz)**.**

- Note that in the present situation the denominator in Equation (18) is one of

$$\frac{2\pi ik}{2\tau} + \alpha\lambda - \lambda_s, \qquad \frac{2\pi ik}{2\tau} + \alpha\lambda - \lambda_u, \qquad \text{or} \qquad \frac{2\pi ik}{2\tau} + \alpha\lambda,$$

  and that none of these are ever zero, due to the assumption that γ is hyperbolic (one stable and one unstable eigenvalue) as well as the condition that $\alpha \geq 2$. Then the solution given by Equation (18) is formally well-defined to all orders. In fact this is a two dimensional stable/unstable manifold of a periodic orbit associated with a single eigendirection. This was already shown in [47] without the use of the Floquet theory and exploited for numerical purposes in [72].

- Note that while Equation (18) gives an explicit representation of the components of the k-th Fourier coefficient of the α-th solution function $v_\alpha(\theta)$ for all k and α, the coefficients $(A_\alpha)_k$ are convolution coefficients depending on the coefficients of $\boldsymbol{R}_\alpha$ and Q^{-1}. Then in fact

$$(A_\alpha)_k = \sum_{\ell\in\mathbb{Z}} (\boldsymbol{R}_\alpha)_{k-\ell}(Q^{-1})_\ell,$$

  and the coefficients of $\boldsymbol{R}_\alpha$ are themselves convolutions involving lower order terms of $\mathbb{P}$. Since we are dealing with Fourier series all of the convolution sums are infinite

series. However in practice we only compute finitely many Fourier coefficients for γ, Q and hence $\boldsymbol{R}_\alpha$.

For example in the Lorenz computations discussed above we have for $\alpha = 2$

$$\boldsymbol{R}_2(\theta) = \begin{pmatrix} 0 \\ -a_1^{(1)}(\theta)a_1^{(3)}(\theta) \\ a_1^{(1)}(\theta)a_1^{(2)}(\theta) \end{pmatrix} = \begin{pmatrix} 0 \\ -\xi^{(1)}(\theta)\xi^{(3)}(\theta) \\ \xi^{(1)}(\theta)\xi^{(2)}(\theta) \end{pmatrix}$$

But $\xi(\theta) = Q(\theta)\xi$ is only known numerically up to K modes, hence $\boldsymbol{R}_2(\theta)$ is only computed approximately. Similar comments apply for all $\alpha \geq 2$, so that all $(A_\alpha)_k$ are only known up to a finite number of terms and (in spite of the exact recursion relations) we only know the functions $v_\alpha(\theta)$ approximately. This makes the a-posteriori analysis discussed in Section 2.6 especially valuable when assessing the quality of the resulting approximation.

- In light of the previous remark we must ask: is the scheme described here at all reasonable? The answer will depend ultimately on the regularity of the vector field f. If f is analytic then γ, Q, and ultimately $\mathbb{P}$ are analytic functions and hence have Fourier-Taylor coefficients which decay exponentially. In this case it is reasonable to expect that some finite number of modes represent the function very well, and that in each convolution term the contributions of higher order modes is not very important.

  On the other hand if f is less regular then this may not be the case and the procedure may fail. These issues are the subject of paper (II). In the present work we focus on analytic vector fields.

2.6 A-Posteriori Error Evaluation

Suppose that

$$P_{NK}(\theta, \sigma) = \sum_{|\alpha|=0}^{N} \sum_{k=-K}^{K} a_k^\alpha e^{\frac{2\pi i k}{2\tau}\theta} \sigma^\alpha,$$

is a candidate solution of Equation (1). Here the coefficients a_k^α may be computed via the techniques of Section (2.4), or by some other method all together (such as in [72]). The natural question is now "how good is the approximate solution P_{NK}?" In order to formalize this question we have to decide on the domain of P_{NK}.

The Question of Domain: *While the global stable/unstable manifold of the periodic orbit is a uniquely defined invariant object, there are many local invariant manifolds. In fact if P is a chart map for $W^{s,u}_{loc}(\gamma)$ and $[0, 2\tau] \times U$ is the domain of P, then P' defined on $[0, 2\tau] \times U'$ is a chart map (for a smaller local stable/unstable manifolds) for any $U' \subset U$ containing the origin. Then when we say that P_{NK} approximates the parameterization map P it is essential that we specify the domain on which the comparison is being made.*

The issue is complicated by the fact that P_{NK} is a trigonometric polynomial, hence the candidate solution is entire. Yet we do not expect that $P_{NK}(\theta, \sigma)$ is a good approximate solution for all $\|\sigma\| > 0$. Rather we expect that there is a $\nu > 0$ so that the approximation is good in the range $0 < \|\sigma\| \leq \nu$.

We employ the following norm when discussing the Fourier-Tyalor series. It is essentially a weighted "little ell one" norm for the space of all sequences of Fourier-Taylor coefficient.

Let

$$\|P\|^W_{r,\nu} = \sum_{|\alpha|\geq 0}\sum_{k\in\mathbb{Z}} \|a^\alpha_k\| e^{\frac{2\pi|k|}{2\tau}r}\nu^{|\alpha|}. \qquad \text{(Weighted Wiener Norm).} \tag{24}$$

It is clear that if this norm is bounded then P has C^0 norm less than $\|P\|^W_{r,\nu}$.

Definition 2.13 (A-Posteriori Error for Equation (8))**.** *Let P_{NK} be an approximate solution of the invariance equation (8). Define the error function of defect associated with P_{NK} to be*

$$E(\theta,\sigma) = \frac{\partial}{\partial\theta}P_{NK}(\theta,\sigma) + D_\sigma P_{NK}(\theta,\sigma)\Lambda\sigma - f\left[P_{NK}(\theta,\sigma)\right],$$

and the a-posteriori error associated with P_{KN} on $\mathbb{A}_r \times \mathbb{D}^k_\nu$ to be

$$\epsilon(r,\nu) = \|E\|^W_{r,\nu}.$$

Supposing that $f \circ P_{NK}$ has Fourier-Taylor expansion

$$f[P_{NK}](\theta,\sigma) = \sum_{|\alpha|\geq 0}\sum_{k\in\mathbb{Z}} b^\alpha_k e^{\frac{2\pi ik}{2\tau}\theta}\sigma^\alpha,$$

we obtain the explicit formula for the a-posteriori error indicator $\epsilon(r,\nu)$ in Fourier-Taylor space given by

$$\epsilon(r,\nu) = \sum_{|\alpha|\geq 0}\sum_{k\in\mathbb{Z}} \left\| \frac{2\pi ik}{2\tau}a^\alpha_k + (\lambda_1\alpha_1 + \ldots + \lambda_k\alpha_k)a^\alpha_k - b^\alpha_k \right\| e^{\frac{2\pi|k|}{2\tau}r}\nu^\alpha. \tag{25}$$

Also note that if f is a polynomial then, since P_{NK} is a trigonometric polynomial, the expression given by Equation (25) reduces to a finite sum. (If f is a non-polynomial analytic vector field then the expression is a finite sum plus a Taylor remainder).

Remark 2.14.

- The utility of Equation (25) in applications is that it gives us a well defined and easy to compute indicator which aids in choosing the numerical domain of approximation. We typically have in mind some fixed value of ϵ as a computational tolerance, and then determine reasonable values of N, K, ν, and $r > 0$ by numerical experimentation.

- Another advantage of using the Wiener-norm framework discussed here is that it sets the stage for the rigorous numerical computations to be taken up in the next paper in this series. We will see that while the choices of function spaces and norms made here are motivated by the desire for efficient numerics, these choices also provide exactly the right theoretical framework for computer assisted validation of the truncation error associated with the approximation of $\mathbb{P}$ by P_{MN}.

- The practical implication of the choice of $\nu > 0$ are easy to see, as this determines the "size" of the image of P_{NK} in phase space. Taking larger values of ν corresponds to parameterizing larger local stable/unstable manifolds. We note that the value of $r > 0$ has somewhat more subtle, but still quite practical implication. r determines the width of the complex strip into which the parameterization can be extended analytically in the time variable. Since analytic bounds on the supremum norm of a function on a complex strip can be traded in for analytic bounds on the derivatives of the function on any smaller strip (via the classical Cauchy bounds), larger values of r correspond to having more control of derivatives with respect to θ. Another way to think of this

is that r controls the decay rates of the Fourier coefficients, i.e. larger values of r correspond to better decay rates for the Fourier coefficients of the manifold. These issues will be essential in the applications to computer assisted proof of connecting orbits between periodic orbits which will be addressed in the second paper in the series.

- The most difficult part of computing $\epsilon(r,\nu)$ is the computation of the Fourier-Taylor expansion of $f \circ \mathbb{P}$. When f is polynomial then the composition may be computed via convolution/Cauchy products. For general nonlinearities the fast Fourier transform can be used in the evaluation. In cases where the vector field is composed of only elementary functions the computation can often be worked out efficiently using the tools of automatic differentiation.

2.7 The case of positive Floquet multiplier

If the stable Floquet multipliers all have positive real part then in fact the stable linear bundle of the periodic orbit is orientable and the parametrization $\mathbb{P}(\theta,\sigma)$ provides a double cover of the invariant manifold. This fact is useful to exploit in practice as it means that the entire manifold is covered by considering only $\theta \in [0,\tau]$ and $\sigma_i \in [-\nu,\nu]$.

2.8 The case of negative Floquet multiplier

As per the discussion in [14] we can have Floquet exponent of the form $\mu = \nu + i\frac{\pi}{\tau}$, giving a characteristic multiplier with negative real part.The characteristic multipliers are the eigenvalues of the monodromy matrix $\Phi(\tau)$ and represent the eigenvalues of the derivative of the Poincare map. Again the geometric interpretation is that the linear bundle, and hence the local invariant manifold, is not orientable.

For the construction of the parametrization, let us consider the real Floquet decomposition of $\Phi(t)$: $\Phi(t) = Q(t)e^{Rt}$ where $Q(t)$ is a 2τ-periodic real matrix function and R is a real matrix. From the properties of the fundamental matrix solution it follows that the real parts of the eigenvalues of B and R coincide.

However the stable/unstable manifold of the τ-periodic orbit $\gamma(t)$ is a τ-periodic geometrical object, then the 2τ-periodic parametrization $\mathbb{P}(\theta,\sigma)$ should cover twice the same manifold.

In practice then

$$\mathbb{P}(\theta+\tau,\sigma) = \mathbb{P}(\theta,\sigma) \qquad \text{or} \qquad \mathbb{P}(\theta+\tau,\sigma) = \mathbb{P}(\theta,-\sigma).$$

The first holds when $Q(t)$ is τ-periodic and the normal bundle is orientable. If it is not the case, it has to be the second.

The relation $\mathbb{P}(\theta+\tau,\sigma) = \mathbb{P}(\theta,-\sigma)$ means

$$\sum_{n\geq 0} a_n(\theta+\tau)\sigma^n = \sum_{n\geq 0} a_n(\theta)(-\sigma)^n.$$

For this it suffices

$$a_n(\theta+\tau) = a_n(\theta), \qquad n \text{ even}$$
$$a_n(\theta+\tau) = -a_n(\theta), \qquad n \text{ odd}$$

that is, a_n is τ periodic for n even and a_n is 2τ periodic but odd in $\theta = \tau$ for odd n. The function $a^0 = \gamma$ and a^1 satisfy the condition.

In practice our computations result in a sequence of a_n with exactly the above properties. Thus we can restrict to positive σ and $\theta \in [0, 2\tau]$ or $\sigma \in [-\delta, \delta]$ and $\theta \in [0, \tau]$ in order to parameterize the complete manifold.

2.9 The case of complex conjugates Floquet multipliers

Consider the case of a complex conjugate pair of stable Floquet multipliers

$$\lambda_{1,2} = a \pm ib.$$

In this case we still conjugate to the flow given by Equation 4, however we do not obtain real results when we flow by

$$e^{\Lambda t}\sigma = \exp\left(\begin{bmatrix} a+ib & 0 \\ 0 & a-ib \end{bmatrix} t\right) \begin{bmatrix} \sigma_1 \\ \sigma_2 \end{bmatrix}.$$

Because of this the coefficients of the parameterization $\mathbb{P}$ will not be real either. Note however that the linear flow still takes complex conjugate arguments to complex conjugate results. This property is then inherited by the parameterization coefficients and is then exploited to obtain a real result.

Making the usual complex conjugate variables $\sigma_1 = t + is$ and $\sigma_2 = t - is$ we observe, by considering the recurrence Equations (18), that the coefficients a_{mn} for the parameterization have that property that

$$a_{nm}(\theta) = \overline{a_{nm}(\theta)}.$$

Then, as long as we have chosen complex conjugate eigenvectors, the complex conjugate change of variables are precisely what is needed in order to obtain a real valued function, i.e,

$$P(\theta, s + it, s - it) \in \mathbb{R}^d$$

for all θ, s, t. This is the same idea used in [56, 57, 61] in order to parameterize real invariant manifolds associated with fixed points when there are complex conjugate eigenvalues. See the works just cited for more thorough discussion.

Finally we note that wether or not the associated linear bundles are orientable will still depend on the sign of the real part of the Multipliers. Yet even in the case of a complex conjugate pair with negative real part/non orientable local manifold, the discussion from Section 2.8 goes through as before and we can parameterize the full real manifold.

3 Numerical Computation of Invariant Manifolds

3.1 A Case Study: A-Posteriori Error and the Lorenz Computations

We are now ready to provide the details for the computations illustrated in Figures 1 and 2. As mentioned in the captions, the figures illustrate local stable/unstable manifolds for a hyperbolic periodic orbit which lies inside the Lorenz attractor at the classical parameters. Performance results for the stable manifold are given in Table 1, while those for the unstable are given in Table 2. Recall that Figures 1 and 2 show the same manifolds from different angles with the stable in red and the unstable in blue. Both manifolds are local, in the sense that no integration has been applied in order to globalize the manifolds.

Both tables list the Taylor order N, the domain parameter $\nu > 0$ (which controls the extent of the local manifold in phase space), the size of the complex strip $r > 0$ used in

N	ν	r	$\epsilon(\nu, r)$	Computation Time	Error Computation Time
2	0.1	0.05	4.39×10^{-6}	0.47 sec	0.008 sec
2	0.1	0.01	7.96×10^{-10}	0.47 sec	0.008 sec
4	0.5	0.01	7.96×10^{-10}	0.82 sec	0.012 sec
10	6	0.01	8.19×10^{-10}	1.83 sec	0.029 sec
20	15	10^{-3}	6.47×10^{-9}	3.57 sec	0.071 sec
25	20	10^{-6}	1.77×10^{-6}	4.42 sec	0.096 sec

Table 1: Some Stable Manifold Performance Data: The periodic orbit, Floquet Normal Form, and all manifold Taylor coefficients $a_n(\theta)$ computed with $K = 66$ Fourier modes.

N	ν	r	$\epsilon(\nu, r)$	Computation Time	Error Computation Time
2	0.1	0.05	4.39×10^{-6}	0.47 sec	0.007 sec
2	0.1	0.01	7.96×10^{-10}	0.47 sec	0.008 sec
4	0.5	0.01	7.96×10^{-10}	0.82 sec	0.012 sec
10	6	0.01	8.67×10^{-10}	1.84 sec	0.03 sec
20	10	10^{-3}	6.12×10^{-9}	3.53 sec	0.071 sec
25	12	10^{-6}	2.39×10^{-7}	4.37 sec	0.097 sec

Table 2: Unstable Manifold Performance Data: Again the Periodic orbit, Floquet Normal Form, and all manifold Taylor coefficients $a_n(\theta)$ are computed with $K = 66$ Fourier modes.

the a-posteriori error error evaluation and the resulting a-posteriori error indicator ϵ. All computations are carried out with 66 Fourier modes. This means that the periodic orbit, the Floquet form, and the solutions of the homological equations for $2 \leq n \leq N$ are computed to 66 Fourier modes. The time taken to compute the parameterization coefficients (i.e. to solve the homological equations for up to order N) as well as the time required in order to evaluate the a-posteriori error are given. We note that the timings do not include the time required in order to compute the Fourier expansion of the orbit and it's Floquet form.

Note that for N large we are able to choose large parameter spaces (for example $6 \leq \nu \leq 20$ on the stable manifold). The local manifolds shown in the figures correspond to those listed in the last lines of the tables, i.e. those computed to the highest order and having the largest parameter domains. The computation of the expansions used in the figures were computed and verified in less than five seconds each.

For ν much larger than shown in the table the a-posteriori errors break down rapidly. Increasing the order does not lead to much improvement. The computations shown in the table/figures are near the point of diminishing return for this problem. We also note that, even in the case of the highest order expansions shown in these tables, the time devoted to evaluation of the a-posteriori error is virtually insignificant compared to the time needed to compute the coefficients. This confirms that once the parameterization is computed to a certain order it is not prohibitively expensive to compute optimal values for ν, r by "guess and check".

3.2 Visualization of the Local Invariant Manifolds

In this section we provide some additional computational results and visualizations. We discuss these computations in less detail than in the previous section. These examples are meant to highlight some situations where our method is applied rather than to give conclusive performance results.

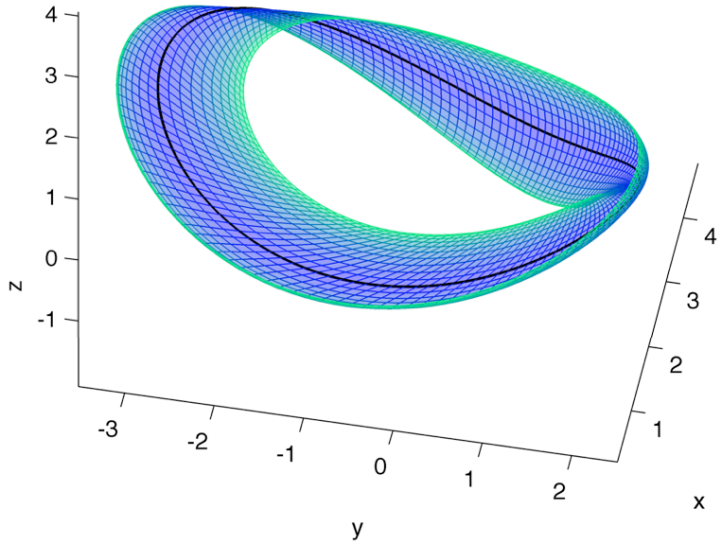

Figure 3: Unstable local manifold of the periodic orbit for the Arneodo system.

Example 1 Consider the Arneodo system,

$$\begin{cases} \dot{x} = y \\ \dot{y} = z \\ \dot{z} = \alpha x - x^2 - \beta y - z. \end{cases} \tag{26}$$

for $\beta = 2$ and $\alpha = 3.372$. It admits a periodic orbit $\gamma(t)$ with period $\tau = 4.5328$. Let us compute the complex Floquet decomposition of the fundamental matrix solution $\Phi(t)$: the exponential matrix B has the following eigenvalues:

$$\lambda_1 = -1.0935 + 0.6931i, \qquad \lambda_2 = 0.0935 + 0.6931i, \qquad \lambda_3 = -0.0000 + 0.0000i.$$

The characteristic multiplier $\sigma_i = e^{\lambda_i \tau}$ are $\sigma_1 = -0.0070$, $\sigma_2 = -1.5275$, $\sigma_3 = 1.0000$. The last one corresponds to the time shift invariance, while the first and the second eigenvalues concern the stable and unstable behavior respectively. Since we are in the case of negative Floquet multipliers, we need to use the 2τ-periodic form for the parametrization of the local manifolds. The local unstable manifold is plotted in figure 3.2, and is very similar to the manifold discussed in [24], with the exception that our manifold is not globalized via numerical integration.

Example 2 The previous examples concerned two dimensional stable/unstable manifolds. Of course the utility of the method is not limited to low dimensional situations. In order to obtain a three dimensional stable manifold we consider the Rössler system,

$$\begin{cases} \dot{x} = -(y + z) \\ \dot{y} = x + \frac{1}{5} y \\ \dot{z} = \frac{1}{5} + z(x - \lambda). \end{cases} \tag{27}$$

For small λ the system has a single fully attracting periodic orbit. As λ is increased the periodic orbit undergoes a period doubling bifurcation giving rise to a chaotic attractor.

We set $\lambda = 0.5$ and compute the periodic orbit and Floquet normal form using 45 Fourier modes. The period of the orbit is roughly $\tau = 5.0832$, and the non-zero multipliers are $\lambda_1 = -0.165772940565187$ and $\lambda_2 = -0.010442224250492$, so the orbit is stable. In this case computing the stable manifold of the orbit provides a trapping region for the orbit on which the dynamics are conjugate to linear. The stable manifold, computed to Taylor order 25, is illustrated in Figure 4.

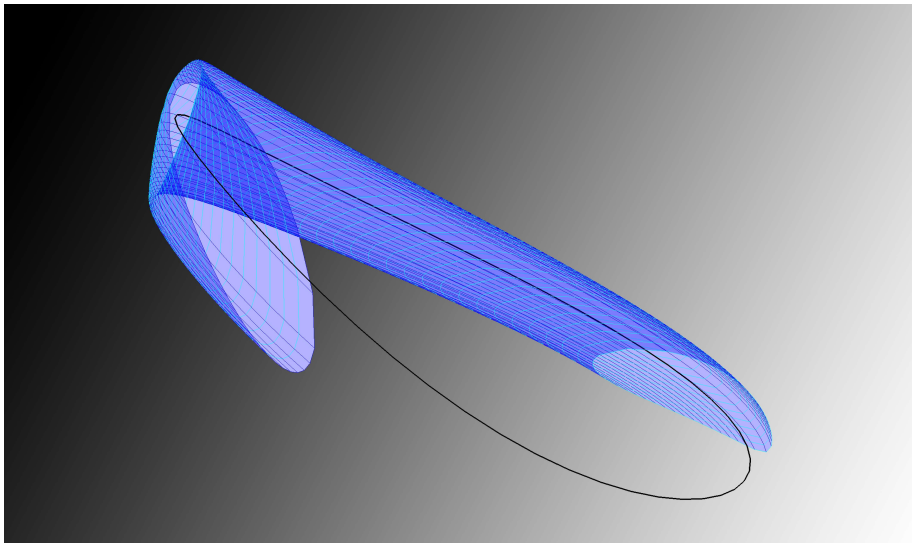

Figure 4: Boundary of a trapping region for the globally attracting periodic orbit of the Rössler system at $\lambda = 0.5$. The manifold is "cut away" in order to show the tubular quality of the trapping region. The trapping region is special in the sense that the dynamics in this tube are conjugate to the linear dynamics given by the Floquet multipliers. The conjugacy is given by our numerically computed parameterization. The tube is the image of a Fourier-Taylor polynomial with $m = 66$ Fourier modes and $N = 25$ Taylor coefficients. No numerical integration is used to obtain this image.

Example 3 In this example we consider a three dimensional stable manifold for an attracting periodic orbit of Lorenz. The result parameterizes a trapping region for the periodic orbit as in Example 2. However the stable manifold in this case is "fast-slow" in the sense that there are three orders of magnitude difference between the Floquet exponents. This leads to a very "flat" trapping region.

We take the Lorenz system with $\rho = 100$, and compute the periodic orbit $\gamma(t)$ with period $\tau = 1.0994$. The complex matrix B in the τ-periodic Floquet decomposition has the following eigenvalues:

$$\lambda_1 = -13.6401 + 2.8575i, \qquad \lambda_2 = -0.0265 + 2.8575i \qquad \lambda_3 = -0.0000 + 0.0000i.$$

Note that $\tau Im(\lambda_1) = 3.1416237$, then the characteristic multiplier $\sigma_1 = e^{\lambda_1 \tau} = -3.070 \cdot 10^{-7}$ is negative. We compute the real Floquet composition $\Phi(t) = Q(t)e^{Rt}$ and it results that the eigenvalues of R are

$$\lambda_1 = -13.6401 \qquad \lambda_2 = -0.0265 \qquad \lambda_3 = -0.0000$$

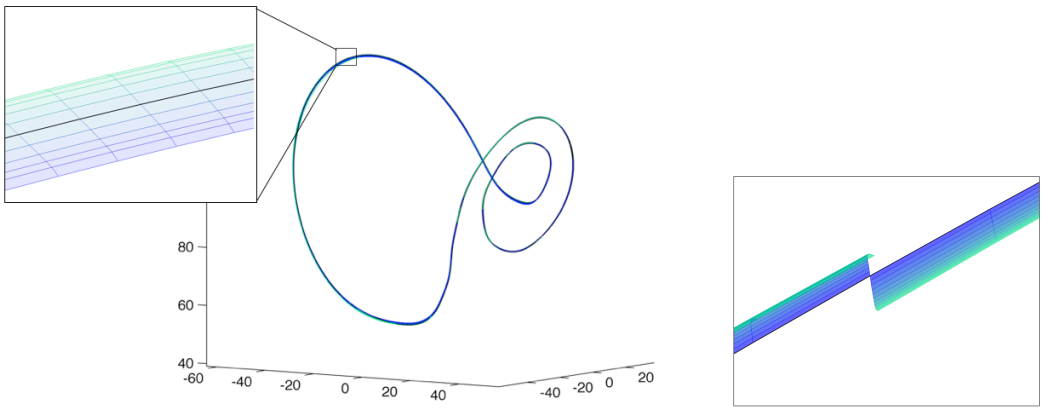

(a) (b)

Figure 5: a) Local stable manifold of an attracting periodic orbit for the Lorenz system with $\rho = 100$ associated to λ_2. Frame b) shows the behavior of the parametrization $\mathbb{P}(\theta, \sigma)$ for $\sigma \in [0, 0.169]$ and $\theta \in [0, \varepsilon) \cup [\tau - \varepsilon, \tau]$, and illustrates that the manifold is not orientable. The color changes with σ, darker blue corresponds to smaller σ.

The orbit is stable as desired. Then, we compute the 2τ periodic parametrization $\mathbb{P}(\theta, \sigma)$ of the manifold associated to λ_2: we obtain a set of functions that agree with the requirement expressed in section 2.8. In Figure 5 the 3-dimensional stable local manifold is depicted for $\theta \in [0, \tau]$ and $\rho \in [-0.168, 0.169]$.

Example 4 We conclude with a higher dimensional example. Consider the Kuramoto-Sivashinsky equation

$$\begin{aligned} &u_t + u_{yy} + \nu u_{yyyy} - 2uu_y = 0 \\ &u(t, y) = u(t, y + 2\pi), u(t, -y) = -u(t, y) \end{aligned} \tag{28}$$

Denoting by $L \overset{\text{def}}{=} \frac{2\pi}{T}$, it follows that the T time periodic solutions can be expanded using the Fourier expansion

$$u(t, y) = \sum_{\boldsymbol{k} \in \mathbb{Z}^2} c_{\boldsymbol{k}} \psi_{\boldsymbol{k}} = \sum_{(k_1, k_2) \in \mathbb{Z}^2} c_{k_1, k_2} e^{iLk_1 t} e^{ik_2 y} \tag{29}$$

for $\boldsymbol{k} = (k_1, k_2) \in \mathbb{Z}^2$ and

$$\psi_{\boldsymbol{k}} \overset{\text{def}}{=} e^{iLk_1 t} e^{ik_2 y}.$$

Instead of considering $k_2 \in \mathbb{Z}$, we may consider a finite dimensional-space reduction of the solution, that is, for a given N, we look for solution of the equation of the form

$$u(t, y) = \sum_{|k_2| \leq N} x_{k_2}(t) e^{ik_2 y} \tag{30}$$

Let us denote by $w_n(t)$ the functions so that $x_n(t) = iw_n(t)$. Then the functions $w_n(t)$ solve the system of ODEs

$$\begin{aligned} \dot{w}_n &= (n^2 - \nu n^4) w_n - n \sum_{k_1 + k_2 = n} w_{k_1} w_{k_2} \\ w_{-n}(t) &= -w_n(t), \quad \forall t, n \end{aligned} \tag{31}$$

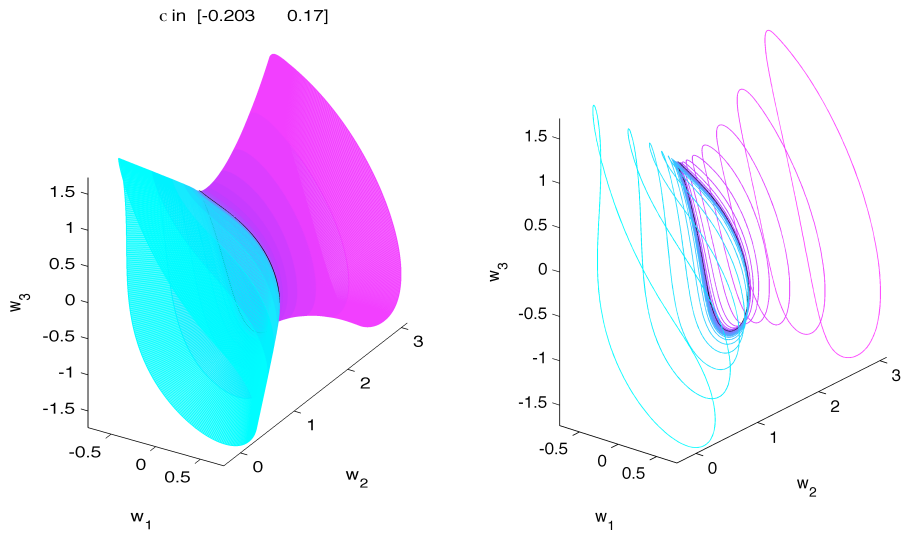

Figure 6: Fast local stable manifold of the periodic solution $w(t)$

For $\nu = 0.1270$ we compute a periodic solution $w(t)$ with period $T = 2.2443$. The orbit is stable, indeed the Floquet exponents (i.e. the eigenvalue of the matrix B in the complex Floquet decomposition of $\Phi(t)$) are

$1.0e+03*$
-1.1691
-0.7513
-0.4558
-0.2555
-0.1281
-0.0535
-0.0147
-0.0021
-0.0000
-0.0006

All the Floquet exponents are negative, hence all the Floquet multipliers $e^{\lambda T}$ have modulus less than one, hence the orbit is stable. Figure 6 shows the projection over the first three variables (w_1, w_2, w_3) of the local stable manifold associated to the last eigenvalue $\lambda_{10} = -0.5730$, i.e. the slow stable manifold of the periodic orbit. This illustrates the fact that the Parameterization Method allows computation of invariant sub-manifolds of the full stable manifold associated with slow eigendirections.

For $\nu = 0.11878$ there is a solution with period $T = 3.894911$. The eigenvalue of B result to be real and one of them is positive: $\lambda = 1.135682$. Hence there is a unstable direction. Figure 7 shows the local unstable manifold.

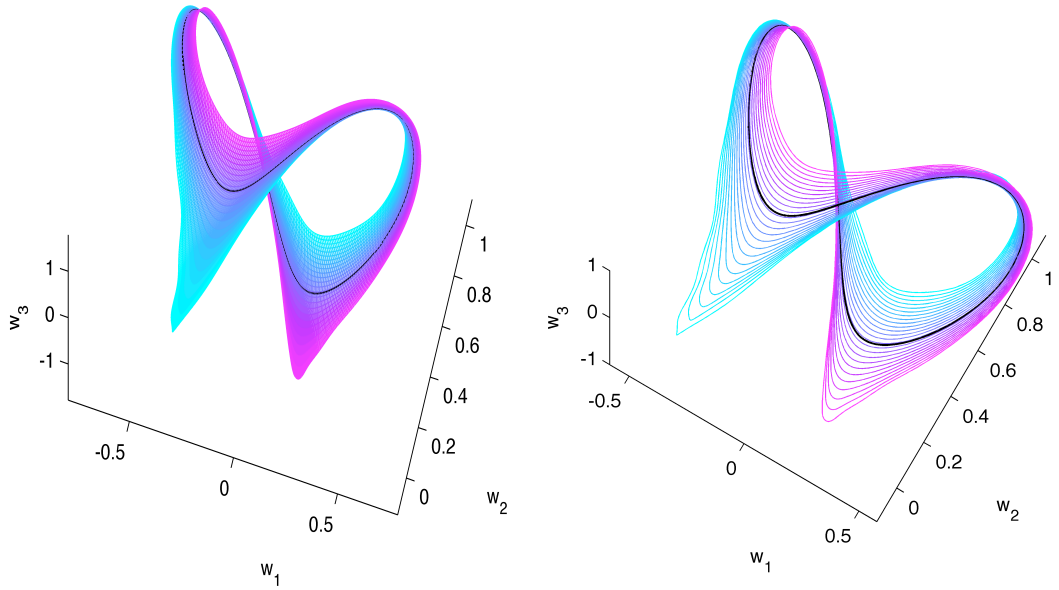

Figure 7: Local unstable manifold of the periodic solution $w(t)$, $\nu = 0.11878$.

4 Preconditioning the Method of Projected Boundary Conditions using Stable/Unstable Manifold Parameterization and Numerical Computation of Connecting Orbits

Local parameterizations of stable and unstable manifolds are useful for computing connecting orbits. The idea is to reformulate the connecting orbit as the solution of a finite time boundary value problem for an orbit segment beginning on the local unstable manifold and terminating on the local unstable. This idea goes back to [29] where it is used in order to compute connecting orbits between equilibria of differential equations. The idea is extended in [31, 32] in order to numerically compute cycle-to-point and cycle-to-cycle connecting orbits.

It is also shown in [30] that high order expansions for the stable/unstable invariant manifolds can be used in order to stabilize the numerical computation of the connecting orbits. Other studies which utilize high order expansions of stable/unstable manifolds in order to study connecting orbits between fixed points and equilibria of discrete time dynamical systems and differential equations are found in [56, 57]. This idea can also be exploited in order to obtain computer assisted proof of the existence of connecting orbits [60, 63, 61]. In this section we discuss some numerical computations for homoclinic connections of periodic orbits exploiting the high order parameterization of the present work.

Let $\gamma_0, \gamma_1 \colon [0, T_{0,1}] \to \mathbb{R}^d$ be hyperbolic periodic orbits for the vector field f, and assume that γ_0 and γ_1 have periods T_0 and T_1 respectively. Suppose in addition that γ_0 has $\lambda^u_1, \ldots, \lambda^u_{k_0}$ unstable eigenvalues, that γ_1 has $\lambda^s_1, \ldots, \lambda^s_{k_1}$ stable eigenvalues, and that $k_0 + k_1 = n - 1$. Now let $P \colon [0, T_0] \times B^{k_0}_{\nu_u} \subset \mathbb{R}^{k_0+1} \to \mathbb{R}^d$ and $Q \colon [0, T_1] \times B^{k_1}_{\nu_s} \subset \mathbb{R}^{k_1+1} \to \mathbb{R}^d$

parameterize the local unstable and stable manifolds, i.e.

$$\text{image}(P) \equiv W^u_{\text{loc}}(\gamma_0) \qquad \text{and} \qquad \text{image}(Q) \equiv W^s_{\text{loc}}(\gamma_1).$$

Furthermore we assume that Q solves Equation (8) with period $T_0 > 0$ and that P solves Equation (8) for the vector field $-f$ and with period T_1. Then P and Q conjugate the dynamics on the stable/unstable manifolds to the linear flows.

The orbit of the point $x_0 \in \mathbb{R}^d$ is *heterocilinic* from γ_0 to γ_1 if

$$\lim_{t \to -\infty} \|\Phi(x_0, t) - \gamma_0(t)\| = 0, \qquad \text{and} \qquad \lim_{t \to \infty} \|\Phi(x_0, t) - \gamma_1(t)\| = 0.$$

If $\gamma_0 = \gamma_1$ then the orbit of x_0 is *homoclinic* for γ_0. Heteroclinic points are equivalent to intersections of stable and unstable manifolds. Note that $\dim(W^s(\gamma_0)) = k_0 + 1$, $\dim(W^u(\gamma_1)) = k_1 + 1$, and that $\dim(W^s(\gamma_0)) + \dim(W^u(\gamma_1) = n + 1$, and we are in the setting where we can look for generic transverse intersections.

A sufficient condition that the orbit of the point $P(\hat{\theta}_0, \hat{\sigma}_0) \in \mathbb{R}^d$ is homoclinic from γ_0 to γ_1 is that

$$\Phi\left[P(\hat{\theta}_0, \hat{\sigma}_0), \tau\right] = Q(\hat{\theta}_1, \hat{\sigma}_1)$$

Note that this expression has n-components, and $n + 2$ variables $\theta_0, \sigma_0, \theta_1, \sigma_1$, and τ. In order to define map from $\mathbb{R}^d$ into itself we impose that constraint (or phase condition) that $\|\sigma_0\| = R_0 < \nu_u$ and $\|\sigma_1\| = R_1 < \nu_s$. In other words we restrict to the surface of a sphere in parameter space. In this setting, where we compute high order parameterizations of the stable/unstable manifolds, these constraints provide natural phase conditions.

In order to formalize this notion let $S_{0,1} \colon \mathbb{S}^{k_{0,1}-1} \to \mathbb{R}^{k_{0,1}}$ be parameterizations of the $k_{0,1}$-spheres of radii R_0, R_1. Then we define the function $F \colon \mathbb{R}^d \to \mathbb{R}^d$ by

$$F(\theta_0, \phi_0, \tau, \theta_1, \phi_1) = \Phi\left[P(\theta_0, S_0(\phi_0)), \tau\right] - Q(\theta_1, S_1(\phi_1)), \tag{32}$$

and look for solutions of $F(\theta_0, \phi_0, \tau, \theta_1, \phi_1) = 0$. Since the map is now from $\mathbb{R}^d$ to itself we compute solutions using a numerical Newton scheme.

Note that there a many variations on Equation (32). For example of we fix a "time of flight" $\tau > 0$ then we only have to constrain one of the variables $\sigma_{0,1}$. Then we obtain heteroclinic connection by looking for zeros of the function $G \colon \mathbb{R}^d \to \mathbb{R}^d$ defined by

$$G(\theta_0, \phi_0, \theta_1, \sigma_1) = \Phi\left[P(\theta_0, S_0(\phi_0)), \tau\right] - Q(\theta_1, \sigma_1),$$

We also note that both F and G as defined above assume that the flow Φ is explicitly known. In practice however Φ is only approximated by numerical integration.

For the purpose of doing computer assisted proofs it is useful to reformulate the boundary value problem in "integrated" form. This exploits the explicit dependance on the vector field f. For example Equation (32) can be rewritten as the nonlinear operator $F \colon C^0([0, \tau]) \times \mathbb{R}^d \to \colon C^0([0, \tau]) \times \mathbb{R}^d$ given by

$$F[u(t), \theta_0, \phi_0, \theta_1, \phi_1] = \begin{pmatrix} P(\theta_0, S_0(\phi_0)) + \int_0^t f[u(s)]\, ds - u(t) \\ Q(\theta_1, S_1(\phi_1)) - P(\theta_0, S_0(\phi_0)) - \int_0^\tau f[u(s)]\, ds \end{pmatrix}, \tag{33}$$

which is solved for the unknown function $u(t)$ as well as the unknown numbers $(\theta_0, \phi_0, \theta_1, \phi_1)$. The operator is discretized by representing $u(t)$ using splines [63, 61] or also Chebychev series [62].

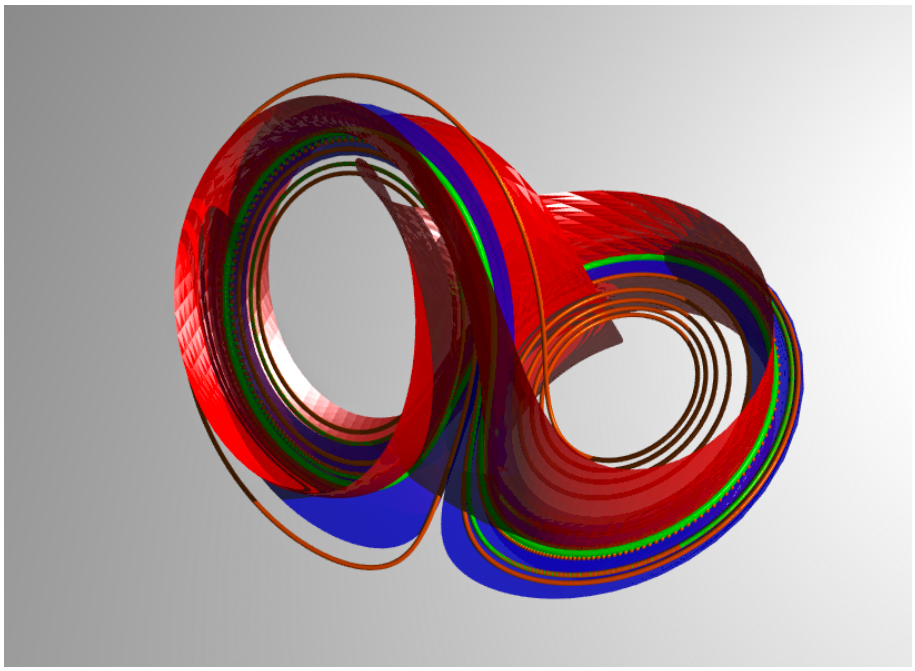

Figure 8: Homoclinic Orbits on the Lorenz Attractor:

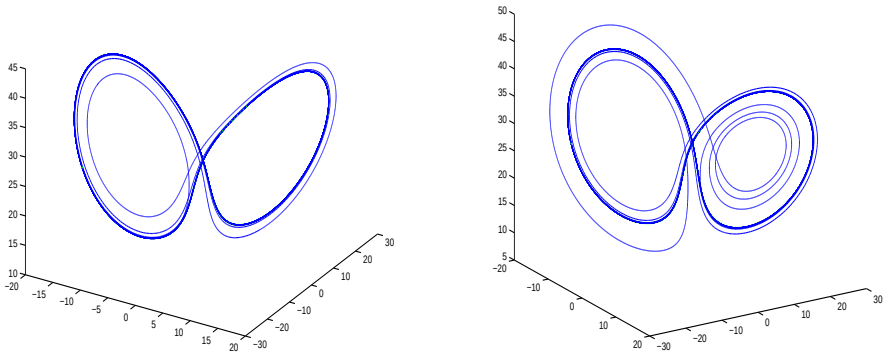

Figure 9: Homoclinic Orbits on the Lorenz Attractor: The figure illustrates two different orbits homoclinic to the same periodic orbit in the Lorenz system. The period of the orbit is $T = 1.4860268$. The "time of flight" for the orbit on the left is $\tau = 1.08145$ while for the orbit in the right we have $\tau = 3.50118$. The boundary conditions are projected onto manifolds of order $N = 15$ computed to $K = 45$ Fourier modes. The orbit on illustrated on the left takes one "turn" around the left lobe of the Lorenz attractor after leaving the local unstable manifold and before returning to the local stable manifold. The orbit on the right on the other hand makes a "turn" on the left lobe of the attractor as well as a number of "turns" on the right lobe during its homoclinic excursion.

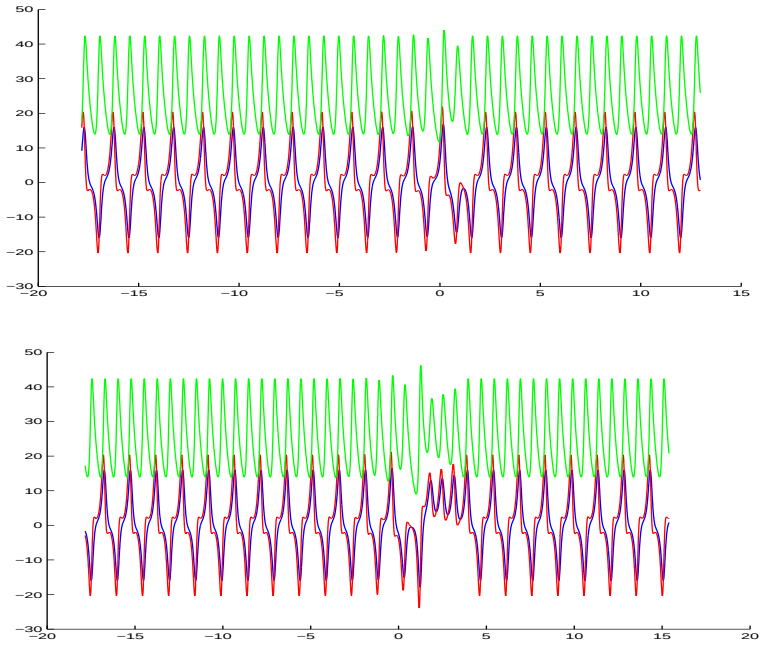

Figure 10: Time Series for Lorenz Homoclinics: The figure illustrates the time series representation of the same homoclinic orbits shown in Figure 4.1. On the left and right hand sides of both the top and bottom orbit the behavior is indistinguishable from periodic. In the middle of both series we see a "wobble" away from the periodic orbit which signifies the homoclinic excursion.

4.1 Numerical Results for Connecting Orbits

First we consider the Lorenz system with parameter values $s = 10$, $\beta = 8/3$, and $\rho = 30$. For these parameters the system is in the chaotic regime. The system is a good place to look for connecting orbits between periodic orbits as hyperbolic periodic orbits are dense on the attractor. Moreover each such periodic orbit has infinitely many homoclinic orbits. Two such homoclinic orbits are illustrated in Figures 4.1 and 4.1. We parameterize the stable/unstable manifolds to Taylor order $N = 25$ and numerically solve Equation (32) using a Newton scheme.

We note that without preconditioning by the parameterized invariant manifolds the method of projected boundary conditions preconditioned requires about 35 time units in order to exhibit their full homoclinic behavior. In other words we see by numerical experimentation that 35 time units is approximately the amount of time required for a homoclinic orbit to start from a small neighborhood of the periodic orbit, make a homoclinic excursion, and return.

On the other hand when we precondition via the parameterized stable/unstable manifolds the numerical integrations required when we solve the boundary value problem for the connecting orbits shown in Figures 4.1 and 4.1 are only $\tau \approx 1.1$ and $\tau \approx 3.5$ respectively. For the remainder of the time the orbits illustrated in the Figures are on the local stable

and unstable manifolds. Then computing these orbits using the linear approximation would require roughly 35 units of integration time, where as the present computations were carried out with less than four. The reader interested in more details of the computations can consult the MatLab programs.

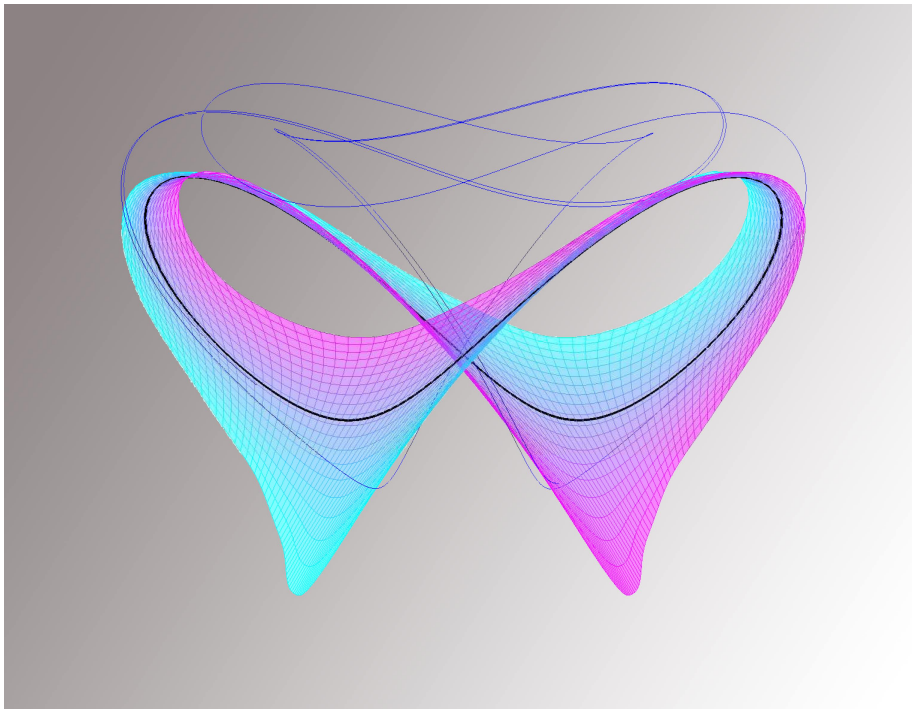

Figure 11: A Homoclinic Orbit in the 10-Dimensional Truncation of Kuramoto-Sivashinsky: The figure illustrates a homoclinic orbit for the PED, truncated to ten modes. The periodic orbit has one unstable direction and eight stable directions. In this computation we use a high order Fourier-Taylor approximation of the unstable manifold, and the linear approximation of the stable manifold provided by the Floquet Normal Form.

Figure (4.1) illustrates a similar computation performed for a hyperbolic periodic orbit of Equation (28). Here we have taken a parameter value of approximately $\nu = 0.119$, and the periodic orbit has period roughly 1.95. This orbit has one unstable direction. The unstable manifold is parameterized using the methods of Section 3. The time of flight for the approximate connecting orbit shown in the Figure is $\tau = 14.5$ time units.

5 Conclusions

6 Acknowledgments

The authors would like to thank Rafael de la Llave for several illuminating discussions. The third author was partially supported by NSF grant DSM 1318172.

References

[1] Marcio Gameiro and Jean-Philippe Lessard. Analytic estimates and rigorous continuation for equilibria of higher-dimensional PDEs. *J. Differential Equations*, 249(9):2237–2268, 2010.

[2] K.E. Davis, R.L. Anderson, D.J. Scheeres, Daniel and G.H. Born. The use of invariant manifolds for transfers between unstable periodic orbits of different energies, *Celestial Mech. Dynam. Astronom.*, Vol. 107, No. 4, 471–485, 2010.

[3] Kathryn E. Davis, Rodney L. Anderson, Daniel J. Scheeres, and George H. Born. Optimal transfers between unstable periodic orbits using invariant manifolds. *Celestial Mech. Dynam. Astronom.*, Vol. 109, No. 3, 241-264, 2011.

[4] D. Blazevski, D. and C. Ocampo. Periodic orbits in the concentric circular restricted four-body problem and their invariant manifolds, *Phys. D*, Vol. 241, No. 13, 1158–1167, 2012.

[5] F. Gabern, A. Jorba, and U. Locatelli. On the construction of the Kolmogorov normal form for the Trojan asteroids, *Nonlinearity*, Vol. 18, No. 4, 1705–1734, 2005.

[6] G. Gómez, J. Llibre, and J.J. Masdemont. Homoclinic and heteroclinic solutions in the restricted three-body problem, *Celestial Mech.*, Vol. 44, No. 3, 239–259, 1988/89.

[7] J. Llibre, R. Martínez, and C. Simó. Tranversality of the invariant manifolds associated to the Lyapunov family of periodic orbits near L_2 in the restricted three-body problem, *J. Differential Equations*, Vol. 58, No. 1, 104–156, 1985.

[8] W. S. Koon, M.W. Lo, J.E. Marsden, and S.D. Ross. Low energy transfer to the moon. *Celestial Mech. Dynam. Astronom.*, Vol. 81, No. 1-2, 63-73, 2000.

[9] G. Gómez, W. S. Koon, M. W. Lo, J. E. Marsden, J. Masdemont, and S. D. Ross. Connecting orbits and invariant manifolds in the spatial restricted three-body problem. *Nonlinearity*, Vol. 17, No. 5, 1571-1606, 2004.

[10] R. Castelli, Regions of prevalence in the coupled restricted three-body problems approximation. *Communications in Nonlinear Science and Numerical Simulation*, Vol. 17, No. 2, 804-816, 2012.

[11] A. Zanzottera, G. Mingotti, R. Castelli, M. Dellnitz, Intersecting invariant manifolds in spatial restricted three-body problems: Design and optimization of Earth-to-halo transfers in the Sun–Earth–Moon scenario. *Communications in Nonlinear Science and Numerical Simulation*, Vol. 17, No. 2, 832-843, 2012.

[12] W. S. Koon, M. W. Lo, J. E. Marsden, and S. D. Ross. Heteroclinic connections between periodic orbits and resonance transitions in celestial mechanics. *Chaos*, Vol. 10, No. 2, 427-469, 2000.

[13] C. Chicone, and W. Liu. Asymptotic phase revisited, *J. Differential Equations*, Vol. 204, No. 1, 227–246, 2004.

[14] C. Chicone, *Ordinary differential equations with applications*, Texts in Applied Mathematics, Vol. 34, 2nd ed., Springer, New York, 2006.

[15] J. Guckenheimer. Isochrons and phaseless sets, *J. Math. Biol.*, Vol. 1, No. 3, 259–273, 1974/75.

[16] F. Gabern, W.S. Koon, S. Wang, J.E. Marsden, and S.D. Ross. Theory and computation of non-RRKM lifetime distributions and rates in chemical systems with three or more degrees of freedom, *Phys. D*, Vol. 211, No. 3-4, 391–406, 2005.

[17] F. Lekien, C. Coulliette, A.J. Mariano, E.H. Ryan, L.K. Shay, G. Haller, and J.E. Marsden. Pollution release tied to invariant manifolds: a case study for the coast of Florida, *Phys. D*, Vol. 210, No. 1-2, 1–20, 2005.

[18] B. Krauskopf, H. M. Osinga, E. J. Doedel, M. E. Henderson, J. Guckenheimer, A. Vladimirsky, M. Dellnitz, and O. Junge. A survey of methods for computing (un)stable manifolds of vector fields. *Internat. J. Bifur. Chaos Appl. Sci. Engrg.*, Vol. 15, No. 3, 763-791, 2005.

[19] J. Guckenheimer and A. Vladimirsky. A fast method for approximating invariant manifolds, *SIAM J. Appl. Dyn. Syst.*, Vol. 3, No. 3, 232–260, 2004.

[20] T. Sahai, and A. Vladimirsky. Numerical methods for approximating invariant manifolds of delayed systems, *SIAM J. Appl. Dyn. Syst.*, Vol. 8, No. 3, 1116–1135, 2009.

[21] M. Dellnitz, and A. Hohmann, Andreas. A subdivision algorithm for the computation of unstable manifolds and global attractors, *Numer. Math.*, Vol. 75, No. 3, 293–317, 1997.

[22] B. Krauskopf, H.M. Osinga. Computing geodesic level sets on global (un)stable manifolds of vector fields, *SIAM J. Appl. Dyn. Syst.*, Vol. 2, No. 4, 546–569, 2003.

[23] B. Krauskopf, and H. Osinga. Two-dimensional global manifolds of vector fields, *Chaos*, Vol. 9, No. 3, 1054–1500, 1999.

[24] H.M. Osinga. Nonorientable manifolds in threee-dimensional vector fields, *Internat. J. Bifur. Chaos Appl. Sci. Engrg.*, Vol. 13, No. 3, 553–570, 2003.

[25] M.E. Johnson, M.S. Jolly, and I.G. Kevrekidis, Ioannis Two-dimensional invariant manifolds and global bifurcations: some approximation and visualization studies, *Numer. Algorithms*, Vol. 14, No. 1-3, 125–140, 1997.

[26] P. Aguirre, E.J. Doedel, B. Krauskopf, H.M. Osinga. Investigating the consequences of global bifurcations for two-dimensional invariant manifolds of vector fields, *Discrete Contin. Dyn. Syst.*, Vol. 29, No. 4, 1309–1344, 2011.

[27] E.J. Doedel, B. Krauskopf, and H.M Osinga. Global invariant manifolds in the transition to preturbulence in the Lorenz system, *Indag. Math. (N.S.)*, Vol. 22, No. 3-4, 222–240, 2011.

[28] Àngel Jorba, and Jordi Villanueva. Numerical computation of normal forms around some periodic orbits of the restricted three-body problem. *Phys. D*, Vol. 114, No. 3-4, 197-229, 1998.

[29] E.J. Doedel, and M.J. Friedman. Numerical computation of heteroclinic orbits, Continuation techniques and bifurcation problems, *J. Comput. Appl. Math.*, Vol 26, No. 1-2, 15–170, 1989.

[30] M.J. Friedman, and E.J. Doedel. Computational methods for global analysis of homoclinic and heteroclinic orbits: a case study. *J. Dynam. Differential Equations*, Vol. 5, No. 1, 37–57, (1993).

[31] E. J. Doedel, B. W. Kooi, G. A. K. van Voorn, and Yu. A. Kuznetsov. Continuation of connecting orbits in 3D-ODEs. I. Point-to-cycle connections. *Internat. J. Bifur. Chaos Appl. Sci. Engrg.* Vol. 18, No. 7, 1889-1903, 2008.

[32] E. J. Doedel, B. W. Kooi, G. A. K. Van Voorn, and Yu. A. Kuznetsov. Continuation of connecting orbits in 3D-ODEs. II. Cycle-to-cycle connections. *Internat. J. Bifur. Chaos Appl. Sci. Engrg.* Vol. 19, No. 1, 159-169, 2009.

[33] R.C. Calleja, E.J. Doedel, A.R. Humphries, A. Lemus-Rodríguez, and E.B. Oldeman. Boundary-value problem formulations for computing invariant manifolds and connecting orbits in the circular restricted three body problem, *Celestial Mech. Dynam. Astronom.*, Vol. 114, No. 1-2, 77–106, 2012.

[34] E. Canalias, and J.J. Masdemont. Homoclinic and heteroclinic transfer trajectories between planar Lyapunov orbits in the sun-earth and earth-moon systems, *Discrete Contin. Dyn. Syst.*, Vol. 14, No. 2, 261–279, 2006.

[35] L. Arona, and J.J. Masdemont. Computation of heteroclinic orbits between normally hyperbolic invariant 3-spheres foliated by 2-dimensional invariant tori in Hill's problem, *Discrete Contin. Dyn. Syst.*, Dynamical Systems and Differential Equations. Proceedings of the 6th AIMS International Conference, suppl. 64–74, 2007.

[36] E.M. Alessi, G. Gómez, and J.J. Masdemont. Leaving the Moon by means of invariant manifolds of libration point orbits, *Commun. Nonlinear Sci. Numer. Simul.*, Vol. 14, No. 12, 4153–4167, 2009.

[37] C. Simó. On the Analytical and Numerical Approximation of Invariant Manifolds. *Les Méthodes Modernes de la Mecánique Céleste* (Course given at Goutelas, France, 1989), 285-329, Editions Frontiéres, Paris, 1990.

[38] A. Jorba, and J.J. Masdemont. Dynamics in the center manifold of the collinear points of the restricted three body problem, *Physica D. Nonlinear Phenomena*, Vol. 132, No. 1-2, 189–213, 1999.

[39] A. Jorba, and J. Villanueva. Numerical computation of normal forms around some periodic orbits of the restricted three-body problem, *Phys. D*, Vol. 114, No. 3-4, 197–229, 1998.

[40] E. Belbruno, M. Gidea, and F. Topputo. Weak stability boundary and invariant manifolds, *SIAM J. Appl. Dyn. Syst.*, Vol. 9, No. 3, 1061–1089, 2010.

[41] E. Belbruno, M. Gidea, and F. Topputo. Geometry of weak stability boundaries. *Qualitative Theory of Dynamical Systems*, Vol. 12, 53-66, 2013.

[42] J.K. Wróbel, and R.H. Goodman, High-order adaptive method for computing two-dimensional invariant manifolds of three-dimensional maps, Commun. Nonlinear Sci. Numer. Simul., Vol. 18, No. 7, 1734–1745, 2013.

[43] R. H. Goodman, and J. K. Wróbel, High-order bisection method for computing invariant manifolds of two-dimensional maps, Internat. J. Bifur. Chaos Appl. Sci. Engrg., Vol. 21, No. 7, 2017–2042, 2011.

[44] W.J. Beyn. The numerical computation of connecting orbits in dynamical systems. *IMA Journal of Numerical Analysis*, vol. 10 (1990), no. 3, 379-405.

[45] X. Cabré, E. Fontich, and R. de la Llave. The Parameterization Method for Invariant Manifolds. I. Manifolds Associated to Non-resonant Subspaces. *Indiana Univ. Math. J.*, 52(2):283-328, (2003).

[46] X. Cabré, E. Fontich, and R. de la Llave. The Parameterization Method for Invariant Manifolds. II. Regularity with Respect to Parameters. *Indiana Univ. Math. J.*, 52(2):329-360, (2003).

[47] X. Cabré, E. Fontich, and R. de la Llave. The parameterization method for invariant manifolds. III. Overview and applications. *J. Differential Equations*, 218(2):444–515, 2005.

[48] D. Viswanath, Divakar, The Lindstedt-Poincaré technique as an algorithm for computing periodic orbits, *SIAM Rev.*, Vol. 43, No. 3, 478–495, 2001.

[49] J.E. Doedel, M.J. Friedman, and A.C. Monteiro, On locating connecting orbits, *Appl. Math. Comput.* vol 65, (1994), no 1-3, 231-239.

[50] B. Krauskopf, and T. Rieß, A Lin's method approach to finding and continuing heteroclinic connections involving periodic orbits. *Nonlinearity*, vol. 21 (2008), no. 8, 1655-1690.

[51] J. Knobloch, and T. Rieß, Lin's method for heteroclinic chains involving periodic orbits, *Nonlinearity*, vol. 23 (2010), no. 1, 23-54.

[52] S. Smale. Diffeomorphisms with Many Periodic Points. 1965 Differential and Combinatorial Topology (A Symposium in Honor of Marston Morse) pp. 63-80 *Princeton Univ. Press*, Princeton, N.J.

[53] D. Wilczak. Abundancs of Heteroclinic and Homoclinic Orbits for the Hyperchaotic Rössler System. *Discrete Contin. Dyn. Syst. Ser. B 11* (2009), no. 4, 1039-1055.

[54] D. Wilczak, and P. Zgliczyński, Heteroclinic connections between periodic orbits in planar restricted circular three body problem. II *Communications in Mathematical Physics*, vol. 259 (2005), no. 3, 561-576.

[55] Jay Mireles-James, Konstantin Mischaikow Rigorous a posteriori computation of (un)stable manifolds and connecting orbits for analytic maps *J. Differential Equations*, 246(5):1774–1819, 2009.

[56] J.D. Mireles James, and Hector Lomelí. Computation of Heteroclinic Arcs with Application to the Volume Preserving Hénon Family. *SIAM J. Applied Dynamical Systems*, Volume 9, Issue 3, pp 919-953, 2010.

[57] J.D. Mireles James Quadratic Volume-Preserving Maps: (Un)stable Manifolds, Hyperbolic Dynamics, and Vortex Bubble Bifurcations. (Submitted).

[58] R. de la Llave, and J.D. Mireles James. Parameterization of Invariant Manifolds by Reducibility for Volume Preserving and Symplectic Maps, (to appear in Discrete and Continuous Dynamical Systems-A)

[59] G. Moore, Floquet theory as a computational tool, SIAM J. Numer. Anal., Vol 42., 2522–2568, 2005.

[60] J.D. Mireles James, and K. Mischaikow, Rigorous a posteriori computation of (un)stable manifolds and connecting orbits for analytic maps, SIAM J. Appl. Dyn. Syst., Vol, 12, No. 2, 957–1006, 2013.

[61] J.P. Lessard, J.D. Mireles James, and C. Reindardt, Computer Assisted Proof of Transverse Saddle-to-Saddle Connecting Orbits for First Order Vector Fields. (Submitted).

[62] J.P. Lessard, and C. Reinhardt. Rigorous numerics for nonlinear differential equations using Chebyshev series. *SIAM Journal on Numerical Analysis*, Vol. 52, No. 1, 1–22, (2014).

[63] J.B. van den Berg, J.D. Mireles-James, J.P Lessard, and K. Mischaikow, Rigorous numerics for symmetric connecting orbits: even homoclinics of the Gray-Scott equation, SIAM J. Math. Anal., Vol. 43, No. 4, 1557–1594, 2011.

[64] J.P. Boyd, *Chebyshev and Fourier Spectral Methods*, 2nd ed., Dover Publications, Inc., New York, 2000.

[65] R. de la Llave. A tutorial on KAM theory, Smooth ergodic theory and its applications (Seattle, WA, 1999), *Proc. Sympos. Pure Math.*, Vol 69, pp. 175-292, 2001.

[66] R. de la Llave, A. González, A. Jorba, and J. Villanueva. KAM theory without action-angle variables, *Nonlinearity*, 18(2) pp. 855-895, (2005).

[67] Á. Haro, and R. de la Llave. A Parameterization Method for the Computation of Invariant Tori and Their Whiskers in Quasi-Periodic Maps: Numerical Algorithms. *Discrete Contin. Dyn. Syst. Ser. B* 6 (2006), no. 6, 1261-1300.

[68] Á. Haro, and R. de la Llave. A Parameterization Method for the Computation of Invariant Tori and their Whiskers in Quasi-Periodic Maps: Rigorous Results. *J. Differential Equations* 288 (2006), no. 2, 530-579.

[69] M. Canadell, and A. Haro. Parameterization method for computing quasi-periodic reducible normally hyperbolic invariant tori, Proceedings CEDYA 2013.

[70] M. Canadell, and A. Haro. A Newton-like method for computing normally hyperbolic invariant tori, *Chapter 5 of Computation of Invariant Manifolds with parametrization methods*, (In progress).

[71] E. Freire, A. Gasull, and A. Guillamon. Limit cycles and Lie symmetries, *Bull. Sci. Math.*, Vol. 131, No. 6, 501–517, 2007.

[72] A. Guillamon and G. Huguet. A Computational and Geometric Approach to Phase Resetting Curves and Surfaces. *SIAM Journal on Applied Dynamical Systems*, Vol 8, Issue 3, pp. 1005-1042 (2009).

[73] E. Fontich, R. de la Llave, and Y. Sire. A Method for the Study of Whiskered Quasi-Periodic and Almost-Periodic Solutoins in Finite and Infinite Dimensional Hamiltonian Systems. *Electronic Research Announcements in Mathematical Sciences* Vol 16, pp. 9-22, (2009).

[74] R. Calleja, and R. de la Llave. Fast Numerical Computation of Quasi-Periodic Equilibrium States in 1D Statistical Mechanics, Including Twist Maps. *Nonlinearity* 22 (2009), no. 6, 1311-1336.

[75] R. Calleja, and R. de la Llave. A Numerically Accessible Criterion for the Breakdown of Quasi-Periodic Solutions and its Rigorous Justification. *Nonlinearity* 23 (2010), no. 9, 2029-2058.

[76] R.C. Calleja, Renato, A. Celletti, and R. de la Llave. A KAM theory for conformally symplectic systems: efficient algorithms and their validation, *J. Differential Equations*, Vol. 255, No. 5, 978–1049, 2013.

[77] W. Tucker, Robust normal forms for saddles of analytic vector fields, Nonlinearity, Vol. 17, No. 5, 1965–1983, 2004.

[78] T. Johnson, and W. Tucker, Warwick, A note on the convergence of parametrised non-resonant invariant manifolds, Qual. Theory Dyn. Syst., Vol. 10, No. 1, 107–121, 2011.

[79] W. Tucker, The Lorenz attractor exists, C. R. Acad. Sci. Paris Sér. I Math., Vol. 328, No. 12, 1197–1202, 1999.

[80] R. Castelli, J.-P. Lessard. Rigorous numerics in Floquet theory: computing stable and unstable bundles of periodic orbits. To appear on SIAM J. Appl. Dyn. Syst..

[81] R. Castelli, J.-P. Lessard. A method to rigorously enclose eigenpairs of complex interval matrices. Submitted.

[82] A. M. Fox, and J.D. Meiss. Efficient Computation of Invariant Tori in Volume-Preserving Maps. *Submitted*.

[83] T. Blass, and R. de la Llave. KAM theory for volume-preserving maps. *Submitted*.

[84] E. Canalias, A. Delshams, J.J. Masdemont, and P Roldán. The scattering map in the planar restricted three body problem. *Celestial Mech. Dynam. Astronom.* Vol. 95, No. 1-4, 155-171, (2006).

[85] A. Delshams, J.J Masdemont, and P. Roldán. Computing the scattering map in the spatial Hill's problem. *Discrete Contin. Dyn. Syst. Ser. B* Vol. 10, No. 2-3, 455–483, (2008)

[86] M.J. Capiński, and P. Roldán. Existence of a center manifold in a practical domain around L_1 in the restricted three-body problem. *SIAM J. Appl. Dyn. Syst.* Vol. 11, No. 1, 285–318, (2012)